# Catalytic role of copper in nitric oxide transfer from S-nitrosothiols to low-molecular-weight thiols

***Mihai Ciortea***

*A Thesis in*

*The Department*

*Of*

*Chemistry and Biochemistry*

*Presented in Partial Fulfillment of the Requirements*

*For the Degree of Master of Science*

*At Concordia University*

*Montreal, Quebec, Canada*

*2004*

*Your file Votre référence*
*ISBN: 0-612-94667-3*
*Our file Notre référence*
*ISBN: 0-612-94667-3*

# *Abstract*

**Catalytic role of copper in nitric oxide transfer from S-nitrosothiols to low-molecular-weight thiols**

Mihai Ciortea

In recent years, much attention has been focused on the chemistry and biology of nitric oxide due to the discovery that it plays a key role in a wide variety of physiological processes. It has been suggested that S-nitrosothiols may be directly involved in many of the biological functions of nitric oxide and that they play a role in nitric oxide storage, transport and delivery. The mechanism of nitric oxide transfer from an S-nitrosothiol to a low-molecular-weight thiol or to a protein-based thiol is still unknown. In this work, evidence for a mechanism in which traces of copper play a role in nitric oxide transfer between thiols is presented. A new synthesis for dansyl homocysteine is described and this fluorescent thiol is used as a direct and sensitive nitric oxide-transfer probe. The results demonstrate that redox turnover of copper is required for efficient nitric oxide transfer between low-molecular-weight thiols.

## *Acknowledgments*

I would like to thank my supervisor, Dr. Ann M. English, for providing ideas and guidance which helped me develop the skills needed to work in the research field. I would also like to thank her for her guidance, encouragement and support in the supervision of this thesis.

I would like to thank all of my lab. colleagues for the frequent discussions, suggestions and friendship which helped me to overcome obstacles during the course of my work.

I would like to thank my parents and my brother for their love and endless support of every kind.

## *Table of contents*

## *List of figures and tables*

## *List of abbreviations*

| | |
|---|---|
| **CuZnSOD** | Cu,Zn-superoxide dismutase |
| **d-hCys** | dansyl homocysteine |
| **d-hCys$_2$** | dansyl homocystine |
| **d-hCysNO** | dansyl homocysteine S-nitrosothiol |
| **DDC** | Diethyldithiocarbamate |
| **DTPA** | diethylenetriamine-N,N,N',N",N"-pentaacetic acid |
| **DTT** | dithiothreitol |
| **EDTA** | ethylenediaminetetraacetic acid |
| **ESI-MS** | electrospray ionization mass spectrometry |
| **GSH** | reduced glutathione |
| **GSNO** | S-nitrosoglutathione |
| **GSSG** | oxidized glutathione, glutathione disulfide |
| **hCys** | homocysteine |
| **hCys$_2$** | homocystine |
| **His** | histidine |
| **HPLC** | high-performance liquid chromatography |
| **ICP-MS** | Inductively coupled plasma-mass spectrometry |
| **MS** | mass spectrometry |
| **NADPH** | nicotinamide adenine dinucleotide phosphate |
| **NAP** | N-acetyl-D,L-penicillamine |
| **Neocuproine** | 2,9-dimethyl-1,10-phenanthroline |

| | |
|---|---|
| **NOS** | nitric oxide synthase |
| **PBS** | phosphate saline buffer |
| **PMT** | Photomultiplier tube |
| **RSNO** | low-molecular-weight S-nitrosothiol |
| **SNAP** | S-nitroso-N-acetyl-D,L-penicillamine |
| **TFA** | trifluoroacetic acid |
| **TLC** | thin layer chromatography |

# *Chapter 1 Overview of nitric oxide transfer between thiols*

## 1.1 Nitric oxide

Although the use of glyceryl trinitrate for medicinal purposes dates back more than 150 years, little had been revealed about its physiological mechanism of action before the 1980's. The nitric oxide (NO) released from glyceryl trinitrate *in vivo* has vasodilatatory effects. The surprising and exciting discovery of the multiple roles that NO plays in physiology led to its being chosen as the "Molecule of the Year" by the editors of Science in 1992 (1). Furchgott, Ignarro and Murad earned the Nobel Prize in 1998 for their discovery of "Nitric oxide as a signaling molecule in the cardiovascular system". Being a simple diatomic free radical, NO is one of the smallest molecules found in the body. It is involved in nearly every biological process from controlling blood pressure to neurotransmission. NO has been found to function within the immune system

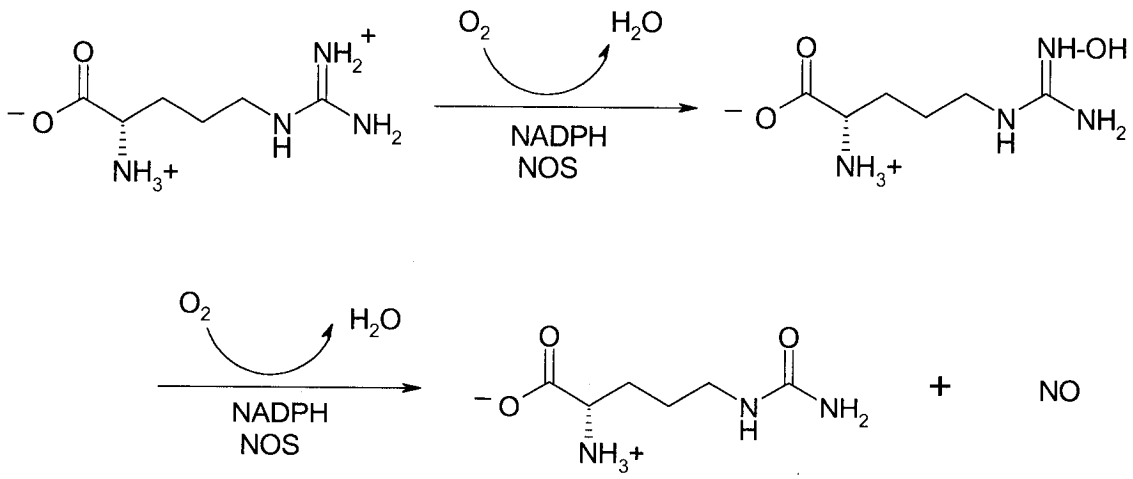


**Figure 1.1 Biosynthesis of NO**

to fight infections, parasites, and tumor cells. In addition, NO has a role in heart disease, hypertension, impotency, shock and cognitive processes (2).

Cellular NO is almost exclusively generated *via* 5-electron oxidation of L-arginine to L-citrulline, catalyzed by nitric oxide synthase (NOS) in the presence of NADPH (Figure 1.1). Nitric oxide is a colorless gas with a solubility of 1-2 mM in water. It undergoes chemical reactions with a variety of molecules and radicals. The reaction with oxygen to generate nitrogen dioxide ($NO_2$) is the best known and one of the most studied reactions of NO, particularly in the gas phase in connection with air pollution caused by nitrogen oxides (3).

$$2NO + O_2 \rightleftharpoons 2NO_2 \rightleftharpoons N_2O_4 \qquad (1.1)$$

$$NO + NO_2 \rightleftharpoons N_2O_3 \qquad (1.2)$$

$$N_2O_3 + H_2O \rightleftharpoons 2NO_2^- + 2H^+ \qquad (1.3)$$

$$N_2O_4 + H_2O \rightleftharpoons NO_2^- + NO_3^- + 2H^+ \qquad (1.4)$$

Reaction (1.1) has a third-order rate constant of ~$5x10^6$ $M^{-1}s^{-1}$ at 25°C, which is unaffected by pH in the range 1-13. At an oxygen concentration of ~ $1x10^{-3}$ M, and a NO concentration of $1x10^{-9}$ M (a typical *in vivo* situation), the half-life of NO is around 50 h, since reaction (1.1) is very slow under these condition. The final product of NO oxidation in aqueous solutions is almost exclusively the nitrite ion, with very little, if any, nitrate ion. The explanation for this is that the reaction of NO with $NO_2$ (eq 1.2) is faster than $N_2O_4$ hydrolysis (eq 1.4). Failure to remove all traces of oxygen from NO solutions can

result in formation of nitrosation products for a number of substrates such as thiols. This led in the biological literature to the erroneous statement that NO itself is an electrophilic nitrosating species (3).

## 1.2 S-Nitrosothiols (RSNOs), NO carriers

S-Nitrosothiols (RSNOs) were less well characterized than their oxygen counterparts, the alkyl nitrites (RONOs), partly due to their relative instability. However, in the last few years there has been an explosion of interest in the chemistry, biochemistry and physiology of RSNOs, the sulfur analogues of alkyl nitrites. The reason for this interest is because RSNOs have similar physiological properties to NO itself. RSNOs have been identified in body fluids, notably S-nitrosoglutathione (GSNO) and S-nitrosoalbumins. The current belief is that NO is transported around the body as RSNO (mostly as S-nitrosoalbumin), from which NO can be released under specific conditions. This belief is based on the short life-time of NO *in vivo* (from a few seconds to a few minutes), whereas RSNOs are generally more stable in solution (3).

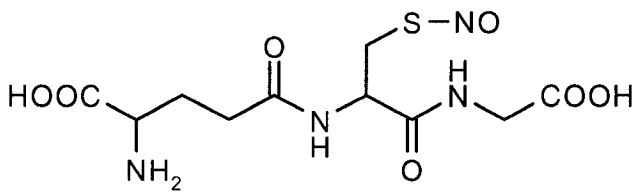


**Figure 1. 2 S-nitrosoglutathione (GSNO),** the most abundant low-molecular-weight RSNO in human fluids

### 1.2.1 *In vitro* synthesis of RSNOs

The first report of RSNO synthesis is from 1840 when a reddish compound was observed upon the treatment of thiols with nitrous acid. Later, more methods were reported starting from thiols (Figure 1.3).

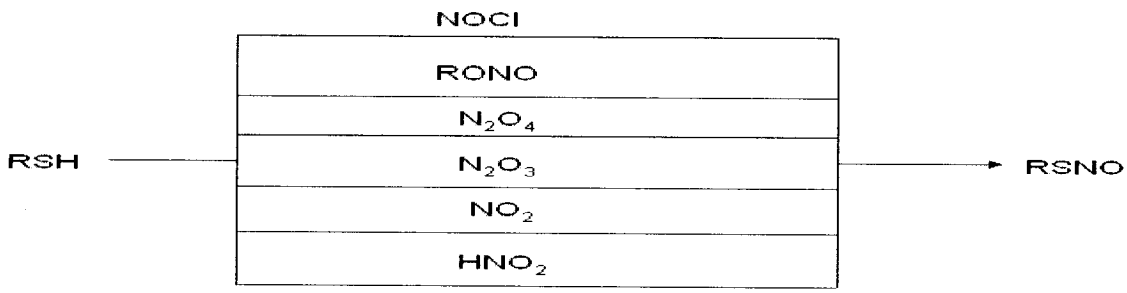


**Figure 1.3 Synthesis of RSNOs from thiols (4)**

The simplest procedure to generate a RSNO from a water-soluble thiol is to add sodium nitrite under mildly acidic solution. The reaction has a yield close to 100% (13) and is relatively easy to handle. In this case, the nitrosating agent is $NO^+$ from $HNO_2$ (eq1.5).

$$RSH + HNO_2 \rightleftharpoons RSNO + H_2O \quad (1.5)$$

In *trans*-S-nitrosation reactions, NO is transferred to another thiol and a new RSNO is generated. Thus, *trans*-S-nitrosation can be considered a method of RSNO synthesis.

$$RSH + R'SNO \rightleftharpoons RSNO + R'SH \quad (1.6)$$

### 1.2.2 Physical and chemical characterization of RSNOs

In general, RSNOs are stable in solution. S-nitroso-N-acetyl-D,L-penicillamine (SNAP) and (GSNO) have been isolated in solid form. However, the **S-N** bond is relatively weak and can be easily broken in a homolytic or heterolytic manner. Studies have shown that homolytic cleavage of the **S-N** bond requires less energy than heterolytic cleavage by ~29 kcal/mol (5).

#### 1.2.2.1 Absorption properties

RSNOs have characteristic UV-vis absorption spectra. In general, they are grey (tertiary RSNO) or red (primary and secondary RSNO) in color. The RSNO absorption spectrum exhibits three bands: two intense bands in UV region and a weak visible band. The band in the 225-261-nm region ($\varepsilon \sim 10^4$ $M^{-1}cm^{-1}$) is attributed to a $\pi \rightarrow \pi^*$ transition. A second band between 330-350-nm ($\varepsilon \sim 10^3$ $M^{-1}cm^{-1}$) is assigned to an allowed $n_O \rightarrow \pi^*$ transition (6). The visible band in the 550-600-nm region ($\varepsilon \sim 20$ $M^{-1}cm^{-1}$) is attributed to a forbidden $n_N \rightarrow \pi^*$ transition, and this determines the RSNO's color (Figure 1.4) (6).

#### 1.2.2.2 Specific reactions of RSNOs

RSNOs undergo many reactions. The most frequently encountered are thermal and photolytic decomposition, metal-catalyzed decomposition and reactions with thiols or protein-based thiols.

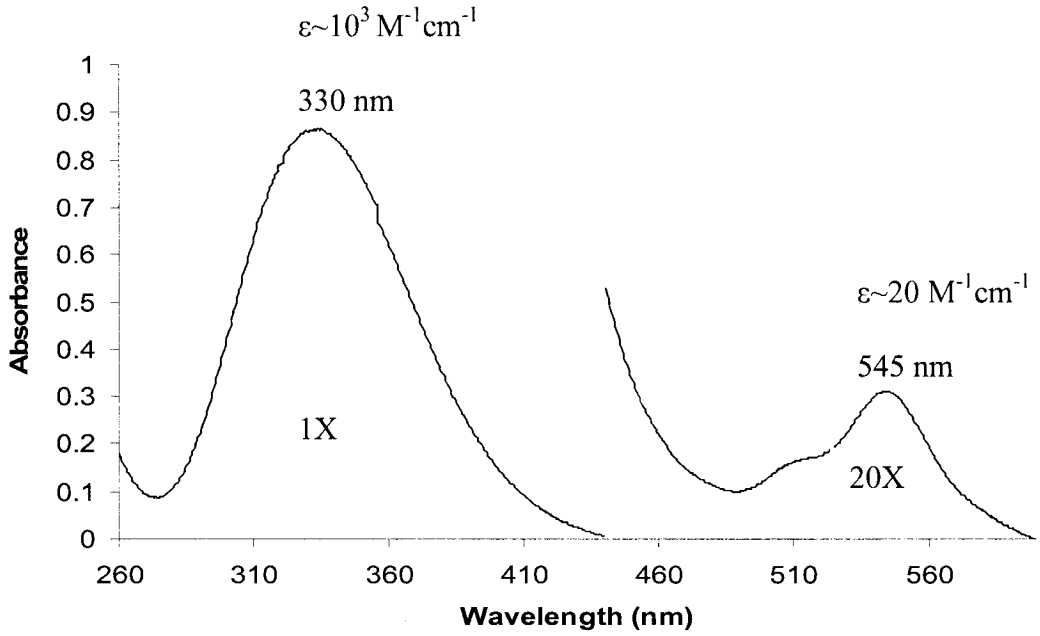


**Figure 1.4 Typical RSNO UV-vis absorption profile.** Due to low absorption at higher wavelength, the signal intensity is multiplied by 20 in the range 450-600 nm

### 1.2.2.2.1 Thermal and photolytic decomposition

RSNOs are sensitive to light (hν) and heat (Δ) and decompose to disulfides and nitric oxide (eq 1.7).

$$\text{RSNO} \xrightarrow{\Delta \text{ or } h\nu} \text{RSSR} + \text{NO} \quad (1.7)$$

The thermal stability of RSNOs shows a wide variation from one compound to another. In the case of S-nitrosocysteine (CysNO), the high decomposition rate prevents isolation of the pure solid (3). On the other hand, solid SNAP has to be heated to about 150°C before significant decomposition occurs (3). In solution in the presence of copper chelators, the decomposition of RSNOs is slow at room temperature in the dark.

Exposure to light in the region where RSNOs absorb (340 or 540 nm) rapidly decomposes them.

Mechanistically, both thermal and photolytic decomposition of RSNOs are reported to be homolytic processes (20):

$$RSNO \rightleftharpoons RS^{\bullet} + NO^{\bullet} \qquad (1.8)$$

$$RS^{\bullet} + RSNO \rightleftharpoons RSSR + NO^{\bullet} \qquad (1.9)$$

RSNO decomposition is also dependent on the presence of oxygen. In aerobic RSNO solutions, the peroxyl radical RSOO (eqs 1.0 and 1.11) was observed suggesting an additional route to NO formation (3):

$$RS^{\bullet} + O_2 \rightleftharpoons RSOO^{\bullet} \qquad (1.10)$$

$$RSOO^{\bullet} + RSNO \rightleftharpoons RSSR + O_2 + NO^{\bullet} \qquad (1.11)$$

#### 1.2.2.2.2 Copper-catalyzed NO release from RSNO

Metals ions can react with RSNOs. Saville reported that $Hg^{2+}$ can release $NO^{+}$ from RSNOs and the Saville method is widely used in the analytical determination of RSNOs (7). Effects of silver and copper ions on RSNOs breakdown are also well known. The reaction with copper is the most biologically relevant, and there are many hypotheses that copper plays a role in NO transfer (3).

Initial studies on RSNO decomposition were irreproducible from one group to another until a study (8) demonstrated that traces of copper catalyze RSNO

decomposition. The report suggested that a copper concentration of ~$10^{-6}$ M could effectively catalyze RSNO decomposition. Such copper concentrations are found in distilled water (8). Thus, when diethylenetriamine-N,N,N',N",N"-pentaacetic acid (DTPA) was added, RSNO decomposition was essentially stopped and addition of excess $Cu^{2+}$ over DTPA re-established RSNO decomposition. Many reports have shown that in copper-catalyzed RSNO decomposition, the active species is $Cu^{1+}$ and not $Cu^{2+}$ although $Cu^{2+}$ is by far the more stable species (E° $Cu^{2+}/Cu^{1+}$=0.15 V) (35). $Cu^{1+}$ is formed under aerobic conditions by *in situ* reduction:

$$Cu^{2+} + RS^- \rightleftharpoons Cu^{1+} + 1/2\ RSSR \qquad (1.12)$$

$$Cu^{1+} + RSNO \rightleftharpoons Cu^{2+} + RS^- + NO \qquad (1.13)$$

Copper-RSNO complexes have been suggested as intermediates in reactions 1.12 and 1.13. However, the structures of the proposed $Cu^{1+}$-RSNO adducts are unknown, but both N and S coordination have been considered (7).

#### 1.2.2.2.3 NO transfer from RSNOs to thiols

*Trans*-S-nitrosation is believed to be a key reaction *in vivo:*

$$R'SH + RSNO \rightleftharpoons R'SNO + RSH \qquad (1.14)$$

Transfer of NO from one RSH to another has been suggested to be a signaling mechanism whereby NO controls cellular processes. The activity of any protein that contains a reduced thiol that is important for activity is likely to be altered by S-nitrosation. This has been shown to occur in the case of glyceraldehyde-3-phosphate

dehydrogenase, creatine kinase and glutathione reductase (7). The first report of the reaction between RSNOs and R'SH *in vitro* indicated the formation of RSSR, RSSR', and R'SSR' as products (8). More recently, it has been suggested that NO transfer from RSNO to R'SH is much faster than copper-catalyzed RSNO decomposition. If the new RSNO is more reactive toward NO formation, it will generate disulfide and NO (8).

The mechanism of *trans*-S-nitrosation is still unknown. NO transfer from RSNO to R'SH is proposed to be a direct process without formation of free NO as an intermediate. This process is reportedly insensitive to copper and follows second-order kinetics (8). The reaction is believed to occur as a result of nucleophile attack of the thiolate anion ($R'S^-$) on the nitrogen of the RSNO (eq 1.15):

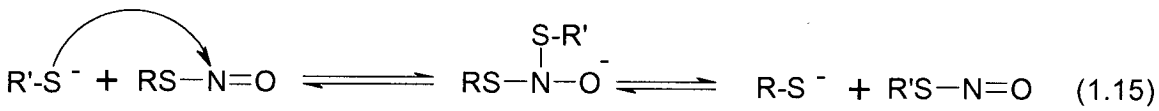


(1.15)

The putative nitroxyl disulfide intermediate, $R'SN(O)SR^-$, in reaction 1.15 was explored computationally (37) and was found to resemble a nitroxyl ($NO^-$) coordinated to a highly distorted disulfide. Evidence from the ESI mass spectrum of SNAP was consistent with the formation of a RSN(O)SR in the gas phase (37). Based on eq 1.15, the thiol $pK_a$ values should be key in controlling the equilibrium of a *trans*-S-nitrosation reaction (9).

Another view considers that copper plays a role in NO transfer. Specifically, $Cu^{1+}$ reductively cleaves the RSNO to release NO, and the NO generated in this way reacts with a thiyl radical. Addition of copper chelators inhibits the redox turnover of copper (21). Recent studies in our lab (17, 18) demonstrate that NO transfer from GSNO to protein thiols requires copper (eqs 1.13, 1.16, 1.17) and is inhibited by chelators:

$$Cu^{1+} + RSNO \rightleftharpoons Cu^{2+} + RS^{-} + NO^{\bullet} \quad (1.13)$$

$$Cu^{2+} + PSH \rightleftharpoons Cu^{1+} + PS^{\bullet} + H^{+} \quad (1.16)$$

$$PS^{\bullet} + NO^{\bullet} \rightleftharpoons PSNO \quad (1.17)$$

## 1.3. Copper,zinc-superoxide dismutase

Many of the experiments that demonstrated a role for copper in RSNO decomposition were performed using hydrated copper present as impurities or copper added as a salt. The total copper in the human body is around 0.1 g and negligible amounts are present as hydrated $Cu^{2+}$ (5). Copper is found in the body bound to proteins. The first report that suggested that protein-bound copper can be reduced to $Cu^{1+}$ and generate NO from RSNO was published in 1996. This report used copper bound to human serum albumin and demonstrated that protein-bound copper can act in a similar manner to free $Cu^{2+}$ (11).

The most abundant known copper protein is the metalloenzyme copper,zinc-superoxide dismutase (CuZnSOD). There are three classes of superoxide dismutases, including manganese superoxide dismutase, which contains a manganese ion and is located exclusively in the mitochondria, iron superoxide dismutase which contains iron and is found in some prokaryotes, and CuZnSOD, which is active in the cytoplasm of eukaryotic cells. CuZnSOD is an essential component of the antioxidant defense of aerobic organisms. Its best characterized function is catalysis of the dismutation of superoxide $(O_2)^-$ to $O_2$ and $H_2O_2$ (eqs 1.18 and 1.19).

$$Cu^{2+} + O_2^- \rightleftharpoons Cu^{1+} + O_2 \qquad (1.18)$$

$$Cu^{1+} + O_2^- + 2H^+ \rightleftharpoons Cu^{2+} + H_2O_2 \qquad (1.19)$$

A key feature of the enzyme is its ability to maintain high dismutase activity while shielding the active-site copper from other redox transformations.

Structurally, CuZnSOD is a dimer of molecular weight 32 kDa. Each monomer contains one $Cu^{2+}$ and one $Zn^{2+}$ ion, and its 151 amino acid residues fold as an eight-stranded Greek-key β-barrel connected by three external loops. The active site of the oxidized ($Cu^{II}$) enzyme consists of a copper and a zinc ion bridged by the imidazolate ring of His61, a feature unique to the enzymes of this class. The $Cu^{II}$ is coordinated by a further three histidine ligands and a water molecule, while Zn is ligated by two additional histidines and an aspartate.

The copper is buried inside the protein. The X-ray structure shows the presence of a narrow channel like a funnel that will accommodate only small anions or ligands. Two positively charged lysines are near the mouth of the channel and are involved in attracting the anions and guiding them through the channel. Arginine in the channel can interact with anions that bind to the copper (12). There is evidence from *in vitro* studies that CuZnSOD plays a role in NO-transfer reactions (32).

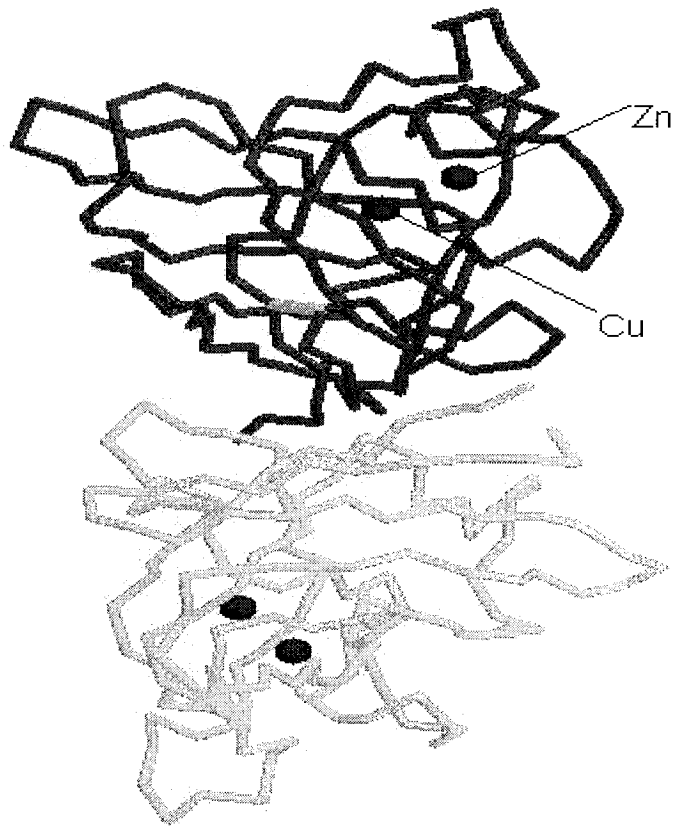


**Figure 1.5 Structure of CuZnSOD** (from http://www.altonweb.com/cs/downsyndrome/sodfig1.gif )

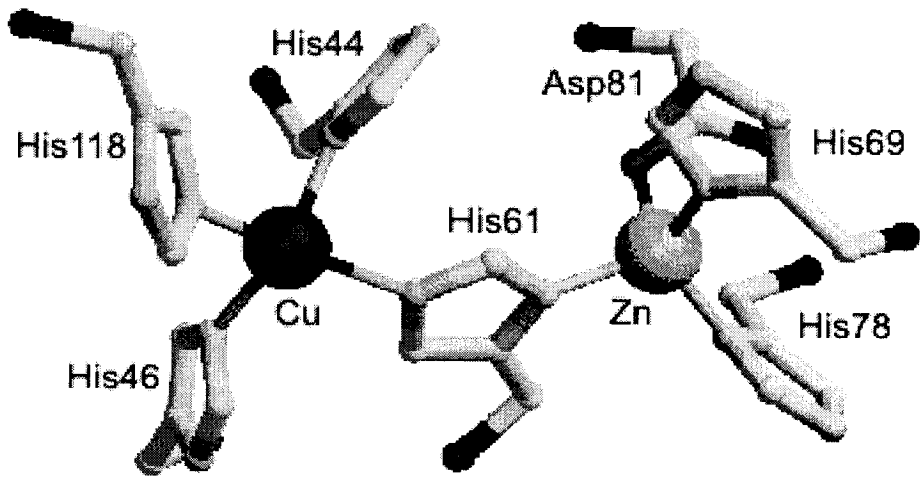


**Figure 1.6 CuZnSOD active site** (from http://www.altonweb.com/cs/downsyndrome/sodfig2.gif)

## 1.4 Dansyl homocysteine (d-hCys), a fluorescent probe for NO release/transfer reactions

Dansyl homocyteine (d-hCys) is an adduct between the amino acid homocysteine (hCys) and the dansyl fluorophore. Dansyl, which is an acronym for 5-**d**imethyl**a**mino-1 **n**aphthalenesulfon**yl**.

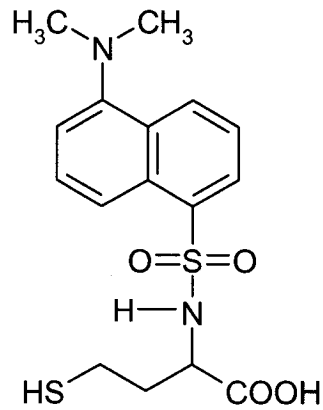


**Figure 1.7 Dansyl homocysteine (d-hCys)**

The dansyl moiety is connected to hCys *via* its free amino group (Figure 1.7). The first report on the quenching of d-hCys fluorescence on its conversion to the RSNO was in 1999 (13). The dansyl moiety exhibits an absorption maximum around 330-360 nm and emits between 530-580 nm, depending on its environment (33). Our measurements show a maximum emission of d-hCys in PBS at 545 nm. The thiol moiety is not affected by dansyl labeling and exhibits thiol-specific reactions allowing d-hCys to be used as a probe of thiol nitrosation. The physical property of d-hCys of interest in this thesis is the fluorescence quenching on its conversion to d-hCysNO (13). The fluorescence variation

during NO addition is a measure of S-nitrosation so d-hCys can be used as a probe for NO-transfer reactions.

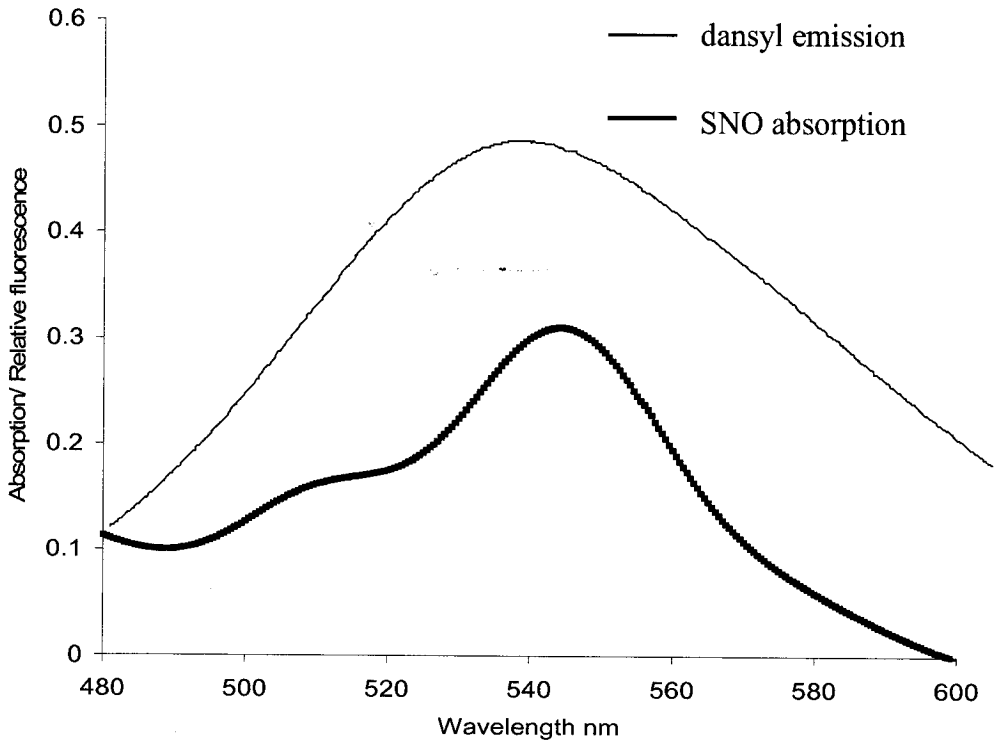


**Figure 1.8 Overlap of SNO absorption and dansyl emission in d-hCysNO.** The SNO absorption was recorded using 100 μM d-hCysNO in PBS (pH 7.4) in a 1-cm cuvette. The emission spectrum of 100 μM d-hCysNO in PBS (pH 7.4) was recorded following excitation at 380 nm with 1-nm excitation slit and 4-nm emission slit.

Quenching is due to the intramolecular energy transfer between the dansyl donor and SNO acceptor (Figure 1.8) . Energy transfer is characterized by the Forster equation:

$$K_T = k^2 J R^{-6} \qquad (1.20)$$

In eq 1.20, $K_T$ is the rate of excited-state energy transfer from a donor to an acceptor; k the relative spatial orientation of the transition dipoles of the donor and acceptor; J the spectral overlap integral of donor and acceptor; and R the donor–acceptor distance.

The overlap integral of SNO absorption and dansyl emission is not enough for efficient energy transfer (25). Hence, the other elements such as donor-acceptor distance and relative spatial orientation of donor and acceptor need to be optimal. As a simplified treatment, it is assumed that only d-hCys conformers with the closest donor-to-acceptor approach dominate the energy-transfer process (25). Quenching will be observed provided that these conformers have reasonable populations (*i.e.,* have energies close to the global minimum).

Calculations using *ab initio* (HF/3-21G) and density functional theory (B3LYP/6-31G) for the free dansyl sulfonamide reveal some interesting features (25). Both N-H bonds of the sulfonamide nitrogen are eclipsed with the S=O bonds, and the rotation of the $SO_2$-$NH_2$ group about the C-S bond is significantly constrained with high rotational barriers due to the steric repulsion between $NH_2$ and naphthalene hydrogens. This suggests that the dansyl sulfonamide unit is fairly rigid, with its S-N bond preferring an orientation out of the plane of the naphthalene. In the case of N-substitution, the terminal group can be oriented either away from or toward the dansyl ring. The energy calculation for both conformers of d-hCysNO reveal that the former conformer is preferred with a distance between the dansyl donor and SNO acceptor of ~4 Å (Figure 1.9).

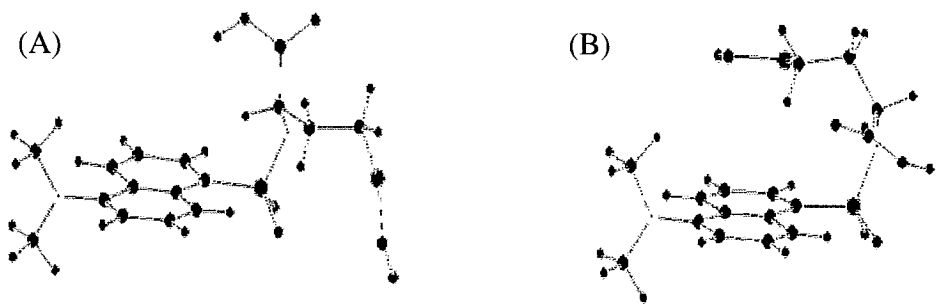


**Figure 1.9 Conformers of d-hCysNO**: (A) "away" conformer and (B) "toward" conformer

## 1.5 Outline of thesis

Recently, our laboratory reported that trace copper catalyzes NO transfer from RSNOs to proteins thiols (17, 18). The effect of copper on NO transfer between low-molecular-weight RSNOs and low-molecular-weight thiols was investigated here. The visible absorbance changes during the reaction of SNAP with GSH and d-hCys (Chapter 2) are compared with the fluorescence measurements during the reaction of GSNO with d-hCys (Chapter 3). Also, in Chapter 3, a new synthesis for d-hCysNO is presented and the compound is used for fluorescence measurements. In Chapter 4, the effects of copper added as either a cuprous (CuCl) or cupric ($CuSO_4$) salt on d-hCysNO stability are investigated by exploiting its fluorescence properties. Likewise, the effects of added CuZnSOD are investigated since our lab has reported that this enzyme catalyzes NO transfer between GSNO and protein thiols. In Chapter 5 a discussion of all the results is given and a mechanism for NO transfer is proposed. A fluorescence screening method for NO acceptors using d-hCysNO is also presented in Chapter 5. In summary, the results reveal that copper catalysis is necessary for NO transfer between low-molecular-weight thiols on a biologically relevant time scale.

# *Chapter 2 Mechanism of NO transfer from SNAP to primary thiols*

## 2.1 Introduction

S-Nitroso-N-acetyl-D,L-penicillamine (SNAP) (Figure 2.1) is a stable RSNO that can serve as a NO donor. The thiol sulfur is connected to a tertiary carbon, so the visible absorption maximum is shifted from 545 nm (characteristic of primary RSNOs) to 590 nm. This red–shift is determined by the *anti* conformation of the R-S-N=O moiety in tertiary RSNOs (23). In primary RSNOs, such as GSNO (Figure 1.2), the preferred conformation is *sin*.

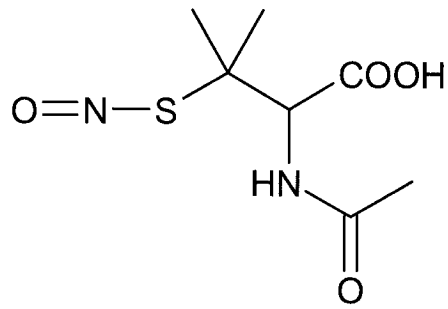


**Figure 2.1 S-nitroso-N-acetyl-D,L-penicillamine (SNAP)**

Since there is a difference in $\lambda_{max}$ between SNAP and primary RSNOs, NO transfer can be directly analyzed using absorbance measurements in the range 510-610 nm. Absorption spectra of mixtures of equimolar SNAP/GSH and SNAP/d-hCysNO were recorded in a quartz cuvette at different time intervals using a Beckman DU-640 spectrophotometer. Since the instrument is equipped with a monochromator for the

emission light, only light with wavelengths between 500-600 nm passed through the sample; thus RSNO photolysis due to exposure to 340-nm light was avoided. The concentration of the reactants and products was monitored *vs* time from the change in SNAP absorption at 590 nm and that of the primary RSNOs at 545 nm. A NO-specific electrode was employed to investigate the free NO levels in the reaction solutions.

## 2.2 Experimental

### 2.2.1 Materials

The synthesis of d-hCysNO is described in Chapter 3. All other reagents were purchased from commercial suppliers and were used as received. S-Nitroso-N-acetyl-D,L-penicillamine (SNAP) was purchased from Cayman Chemical, high purity zinc acetate dihydrate from Fluka, Cu,Zn-superoxide dismutase (CuZnSOD) from Roche, glutathione (GSH), 2,9-dimethyl-1,10-phenanthroline (neocuproine), diethylenetriamine-N,N,N',N",N"-pentaacetic acid (DTPA), ethylenediaminetetraacetic acid (EDTA), diethyldithiocarbamate (DDC) and phosphate saline buffer (PBS) tablets from Sigma; and Tris base from ICN. Water (18.2 MΩ) from a Millipore Simplicity system was used in all solutions. Tris-Cl and PBS buffers were used in all experiments. A solution of 0.01 M Tris base was prepared in 18.2 MΩ water and the pH was adjusted to 7.4 with concentrated HCl. PBS tablets were used to prepare a 0.01 M phosphate solution in 18.2 MΩ water and the pH was adjusted to 7.4 with concentrated HCl.

Both buffers (0.01 M Tris and 0.01 PBS) were treated with 4 g Chelex 100 each to remove all trace of metals. The resin was removed by filtration.

### 2.2.2 Effects of metal chelators

To a solution of 4 mM SNAP in PBS (pH 7.4) with 1 mM (DTPA) in a 1-cm quartz cuvette, an equal volume of 4 mM GSH in the same buffer was added. The absorption spectrum in the range of 520-620 nm was recorded at 5-min intervals over a period of 60 min at room temperature. As a control, readings were recorded for the same solution without GSH.

The absorption experiments were repeated using different chelators as follows: To a solution of 0.6 mM SNAP in Tris buffer (pH 7.4), an equal volume of 0.6 mM GSH in the same buffer was added. DTPA, EDTA, DDC or neocuproine was present in the buffer at a concentration of 50 μM. The visible absorption spectra in range 520-620 nm were recorded at 15-s intervals for a period of 195 s at room temperature. The reaction without any chelators was also studied.

### 2.2.3 Relative efficiencies of DTPA and GSSG as copper chelators

To determine the minimum DTPA concentration necessary to affect NO transfer, 0.6 mM SNAP and GSH were mixed in Tris buffer (pH 7.4). DTPA was added to final concentrations of 2.5 μM, 5 μM, 10 μM, 25 μM, 50 μM and 100 μM and the absorbance between 520-620 nm was recorded at 15-s intervals over 195 s at room temperature. The experiments were repeated replacing DTPA with oxidized glutathione (GSSG) in the following concentrations: 25 μM, 40 μM and 50 μM. The reaction without chelators was run as a control.

### 2.2.4 Effects of added $Zn^{2+}$

In order to investigate if hydrated $Zn^{2+}$ affects the reaction between SNAP and GSH, $ZnAc_2$ was added to final concentrations of 0.016 mM, 0.08 mM and 0.8 mM. Equal volumes of 0.6 mM SNAP and 0.6 mM GSH in Tris buffer (pH 7.4) were mixed and $ZnAc_2$ was added. The reaction without added $Zn^{2+}$ was used as a control. The absorbance between 520-620 nm was recorded at 15-s intervals for a period of 195 s at room temperature. No chelators were present in the buffers.

### 2.2.5 Effects of CuZnSOD

The effect of CuZnSOD on NO transfer from SNAP to the primary thiols, GSH and d-hCys, was investigated. Equal volumes of 0.6 mM SNAP and 0.6 mM GSH or d-hCys in Tris (pH 7.4) were mixed. Where indicated, 8.3 μM CuZnSOD was added just before the primary thiol and the absorbance between 510-610 nm was recorded each 15 s over 360 s. For the reactions in the presence of chelators, buffers containing 100 μM DTPA or 100 μM neocuproine were used.

### 2.2.6 Amperometric determination of free NO in SNAP/GSH solutions

NO levels were recorded using an ISO-NO MARK II Nitric Oxide Meter with a NO-specific electrode. The meter was calibrated using the method described by the manufacturer (38). A 600-μL aliquot of 0.5 mM GSH in Tris buffer (pH 7.4) was added to a 2-mL brown Eppendorf tube (to protect the sample from light) with a magnetic stir

bar. The NO-electrode was dipped into the thiol solution and the electrode was equilibrated each time for 1 min before addition of SNAP to a final concentration of 0.5 mM in the same buffer. The NO levels were measured over 360 s. CuZnSOD was added to a final concentration of 5 μM just before SNAP addition where indicated.

## 2.3 Results

### 2.3.1 Effects of metal chelators

In an equimolecular solution of SNAP and GSH containing 1 mM DTPA, the 590-nm band of SNAP decreases and the GSH band at 545-nm increases *vs* time (Figure 2.2). After 60 min the change between two consecutive spectra is negligible and it is assumed that the equilibrium state has been reached (Figure 2.2). Both SNAP and GSNO are present in the equilibrium mixture. The control (without GSH), shows no change in 590-nm intensity over 60 min (Figure 2.3), demonstrating that the decrease is due to the presence of GSH and that no SNAP photolysis occurred in this time interval.

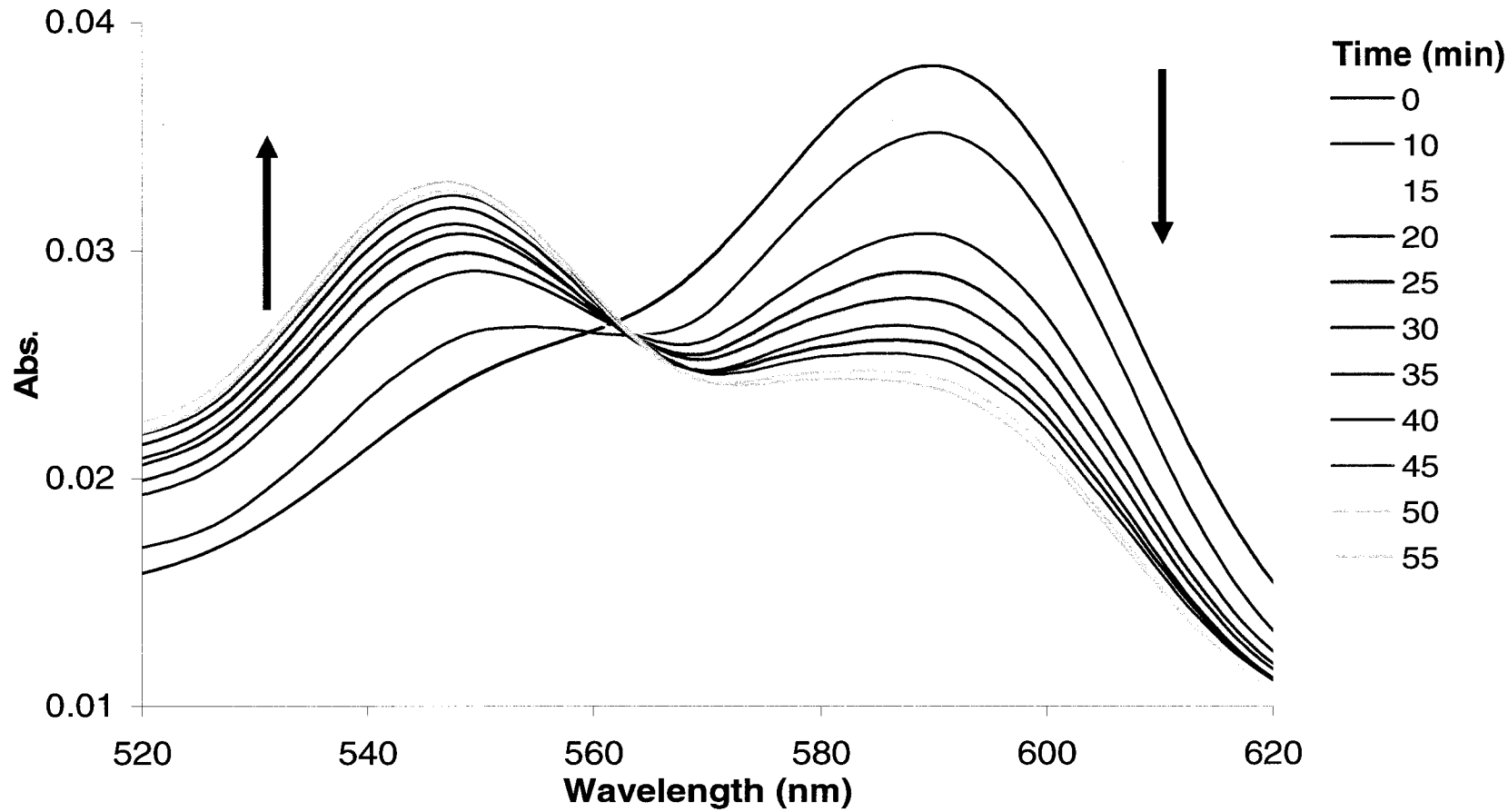


**Figure 2.2 Spectral changes during the incubation of 1.99 mM SNAP and 2.00 mM GSH in PBS/1 mM DTPA (pH 7.4) at room temperature**. Spectra recorded in a 1-cm cell, at 5-min intervals from t=0 to 55 min are shown. The arrows indicate that the band at 545 nm grows in at the expense at the 590-nm band.

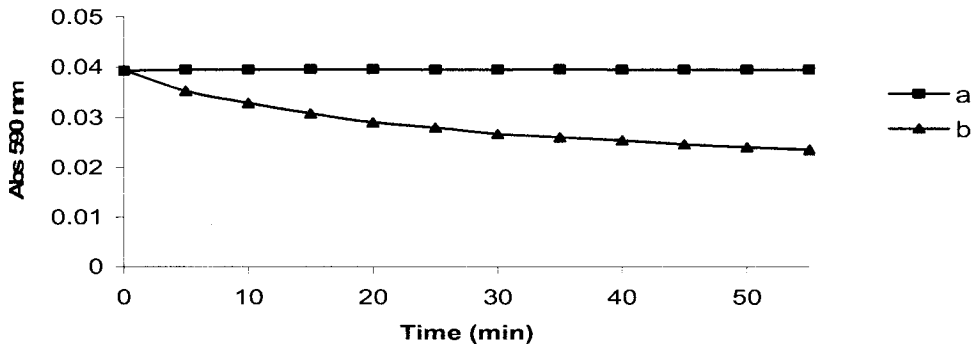


**Figure 2.3 Time course of the absorbance change at 590 nm in a solution of 1.99 mM SNAP ± 2.00 mM GSH in PBS/1 mM DTPA (pH 7.4) at room temperature.** (a) 1.99 mM SNAP only; (b) 1.99 mM SNAP + 2.00 mM GSH. See legend of Figure 2.2 for experimental details.

The reaction between 0.29 mM SNAP and 0.29 mM GSH in Tris buffer (pH 7.4) in absence of chelators at room temperature was also monitored. An initial strong absorption at 590 nm was observed. This SNAP band rapidly decreased and disappeared completely after 180 s while the 545-nm band grew in (Figure 2.4). However, in the presence of different chelators, there was little detectable loss of absorption at 590 nm or growth of absorption at 545 nm over the first 3 min (Figures 2.5 and 2.6). Neocuproine, a $Cu^{1+}$-specific chelator inhibits the reaction as do the $Cu^{2+}$ specific chelators, DTPA, EDTA and DDC.

The data in Figure 2.5 clearly show that copper catalyzes NO transfer between SNAP and GSH. From the calculated molar absorptivities for GSNO ($\varepsilon_{590} = 0.238\ M^{-1}cm^{-1}$, $\varepsilon_{545} = 17.2\ M^{-1}cm^{-1}$) and SNAP ($\varepsilon_{545} = 11.59\ M^{-1}cm^{-1}$, $\varepsilon_{590} = 19.045\ M^{-1}cm^{-1}$), 1.99 mM SNAP is converted to 1.07 mM GSNO in 55 min, and equilibrium concentrations of 1.07 mM GSNO and 0.87 mM SNAP appear to be established after 1 h in the presence of 1 mM DTPA (Figure 2.2). However, in the absence of chelators, no SNAP remains in solution after 3 min and 0.296 mM GSNO is present (Figure 2.4).

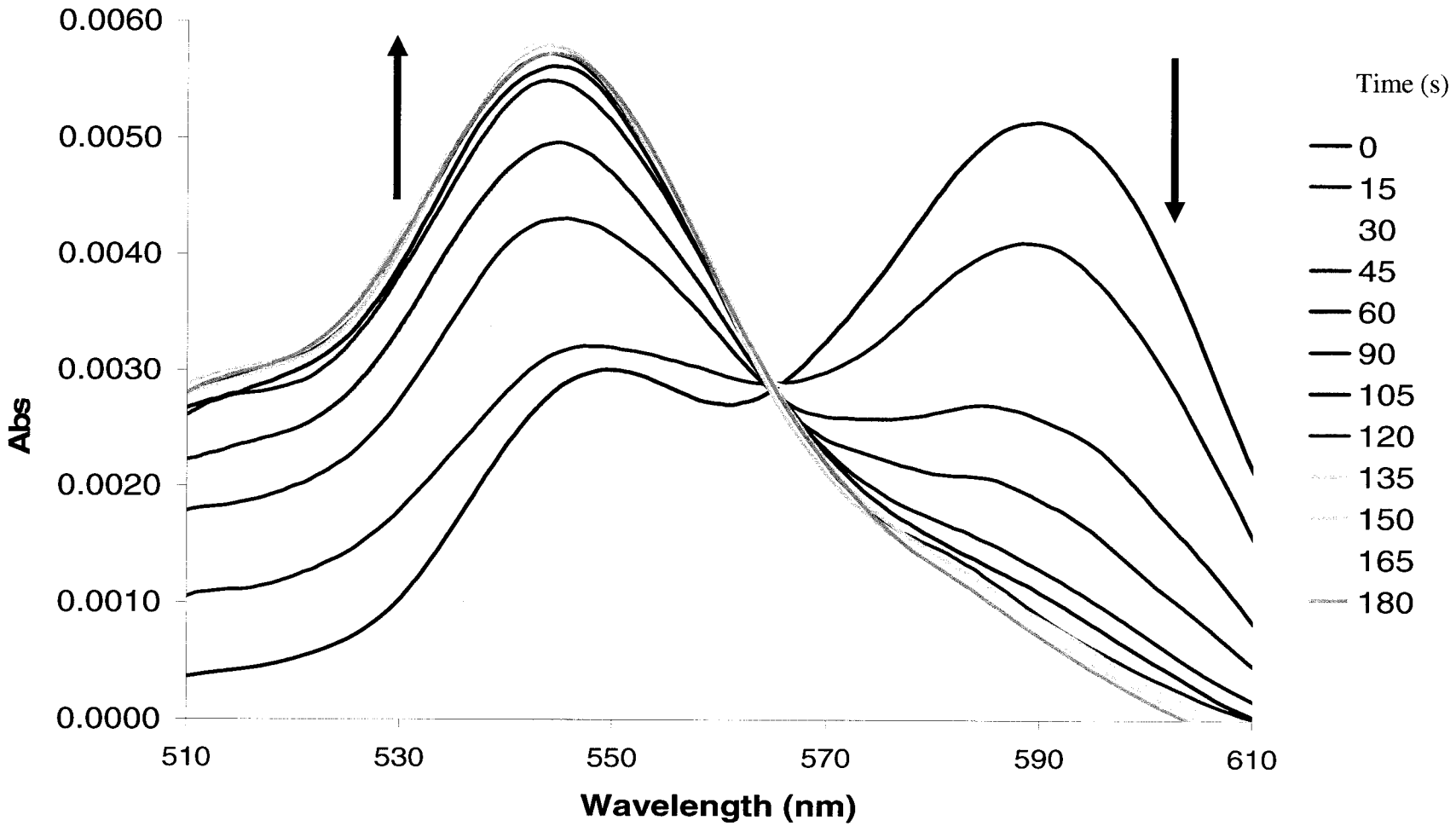


**Figure 2.4 Spectral changes during the incubation of 0.299 mM SNAP with 0.297 mM GSH in Tris buffer (pH 7.4) at room temperature in absence of metal chelators.** Spectra recorded in a 1-cm cell at 15-s intervals up to 180 s are shown.

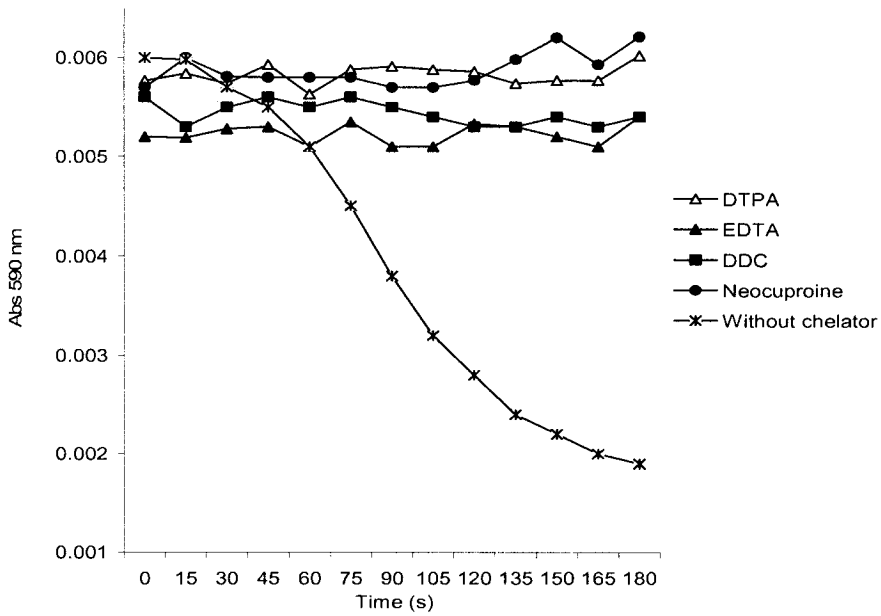


**Figure 2.5 Time course of the absorbance change at 590 nm during incubation of 0.299 mM SNAP and 0.297 mM GSH in Tris buffer (pH 7.4) at room temperature.** Chelator concentrations were 50 μM.

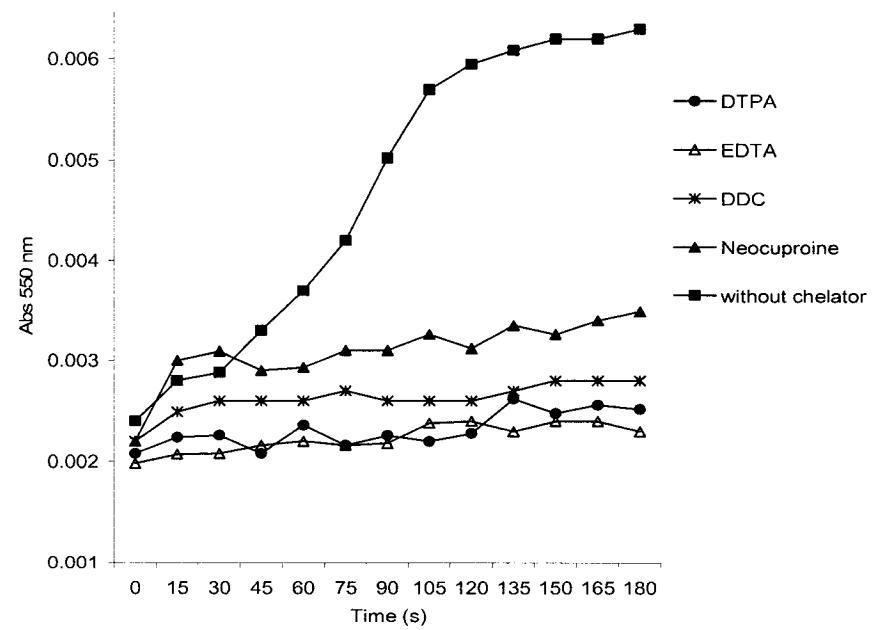


**Figure 2.6 Time course of the absorbance change at 545 nm during the incubation of 0.299 mM SNAP and 0.297 mM GSH in Tris buffer (pH 7.4) at room temperature.** Chelator concentrations were 50 μM.

### 2.3.2 Relative efficiencies of DTPA and GSSG as copper chelators

The reaction between SNAP and GSH was carried out in the presence of different DTPA concentrations to investigate the minimum concentration necessary to inhibit copper-catalyzed NO transfer. The results demonstrate that 2.5 - 5 μM DTPA partially inhibits copper-catalysis and ≥ 5 μM DTPA fully inhibit the catalysis over 3 min (Figure 2.7). The results are consistent with the determination of copper in our lab. Using inductively-coupled plasma mass spectrometry (ICP-MS), 1 μM copper was found in the water from the Millipore system (17).

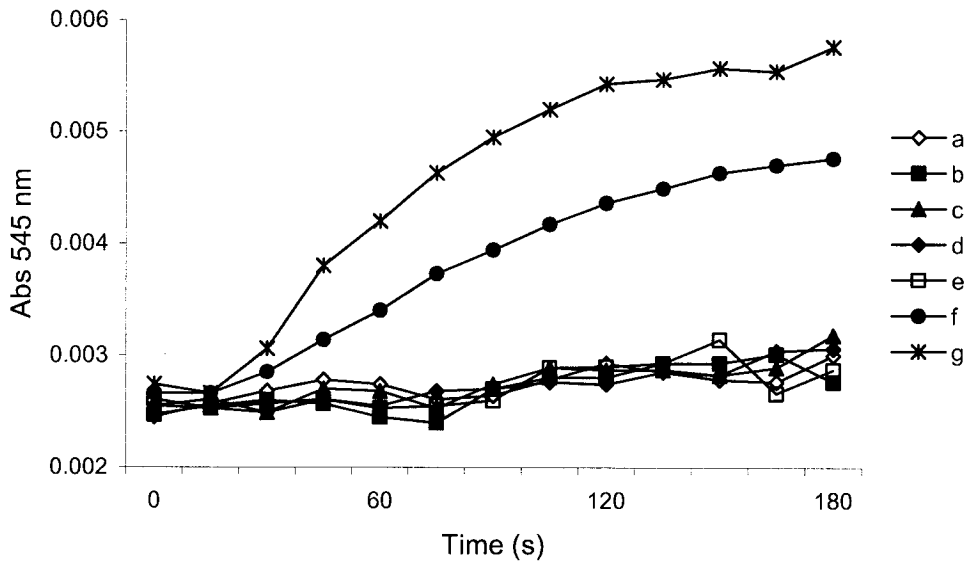


**Figure 2.7 Time course of the absorbance change at 545 nm during incubation of 0.299 mM SNAP and 0.297 mM GSH *vs* DTPA concentrations** The DTPA concentrations were: (a) 100 μM, (b) 50 μM, (c) 25 μM, (d) 10 μM, (e) 5 μM, (f) 2.5 μM, and (g) no chelator. Samples were in PBS (pH 7.4) and incubated for 20 min. Absorbances were recorded in a 1-cm cuvette.

Monitoring the reaction between SNAP and GSH in the presence of different concentrations of GSSG as a copper chelator reveals that more GSSG is needed to inhibit copper-catalyzed transfer than DTPA. In the presence of 25 μM GSSG, NO transfer between SNAP and GSH is slowed down, but even at 50 μM GSSG, the copper catalysis of NO transfer is not fully inhibited over 3 min (Figure 2.8).

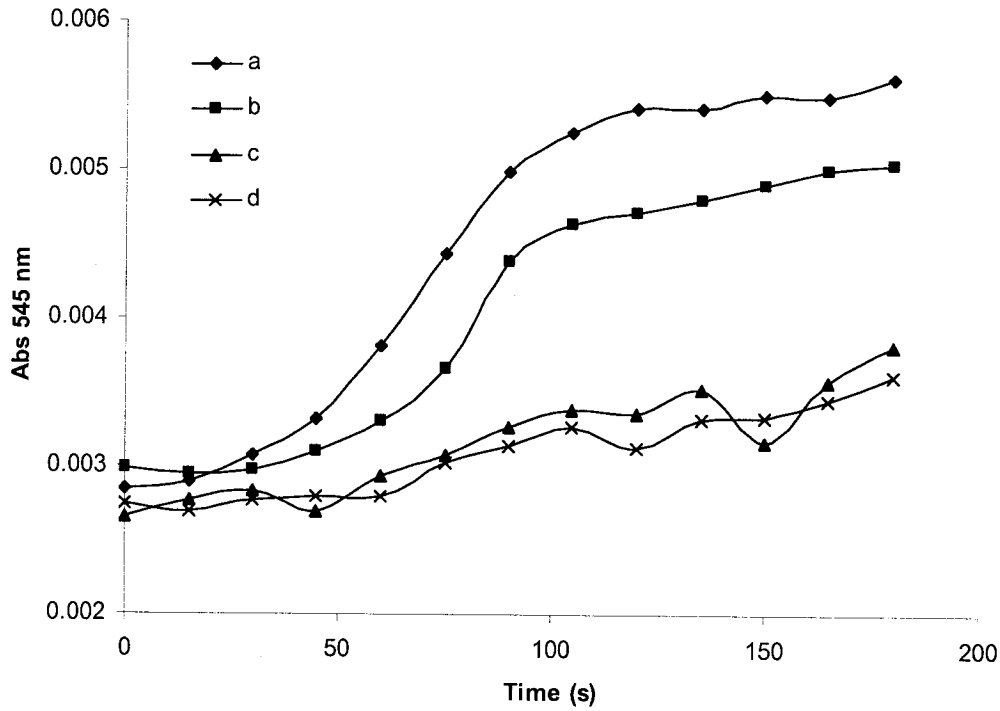


**Figure 2.8 Time course of the absorbance change at 545 nm during incubation of 0.299 mM SNAP and 0.297 mM GSH in PBS at room temperature *vs* GSSG concentration.** The GSSG concentrations were: (a) 0; (b) 25 μM, (c) 40 μM, and (d) 50 μM. The experimental conditions are given in the legend of Figure 2.7

## 2.3.3 Effects of added $Zn^{2+}$

To study the effect of hydrated $Zn^{2+}$ on NO transfer, high purity $ZnAc_2$ was used. The analysis report from Fluka certified a copper content of < 0.0005% in the acetate salt.

Thus, at the highest $Zn^{2+}$ concentration used (0.8 mM), the additional copper present will be <0.13 μM, which is much lower than the 1 μM $Cu^{2+}$ found in the lab water (17). Thus, the copper concentration was essentially unchanged by adding the $Zn^{2+}$ salt. The results demonstrate that addition of up to 0.8 mM $Zn^{2+}$ does not affect NO transfer from SNAP to GSH over ~6 min at room temperature (Figure 2.9).

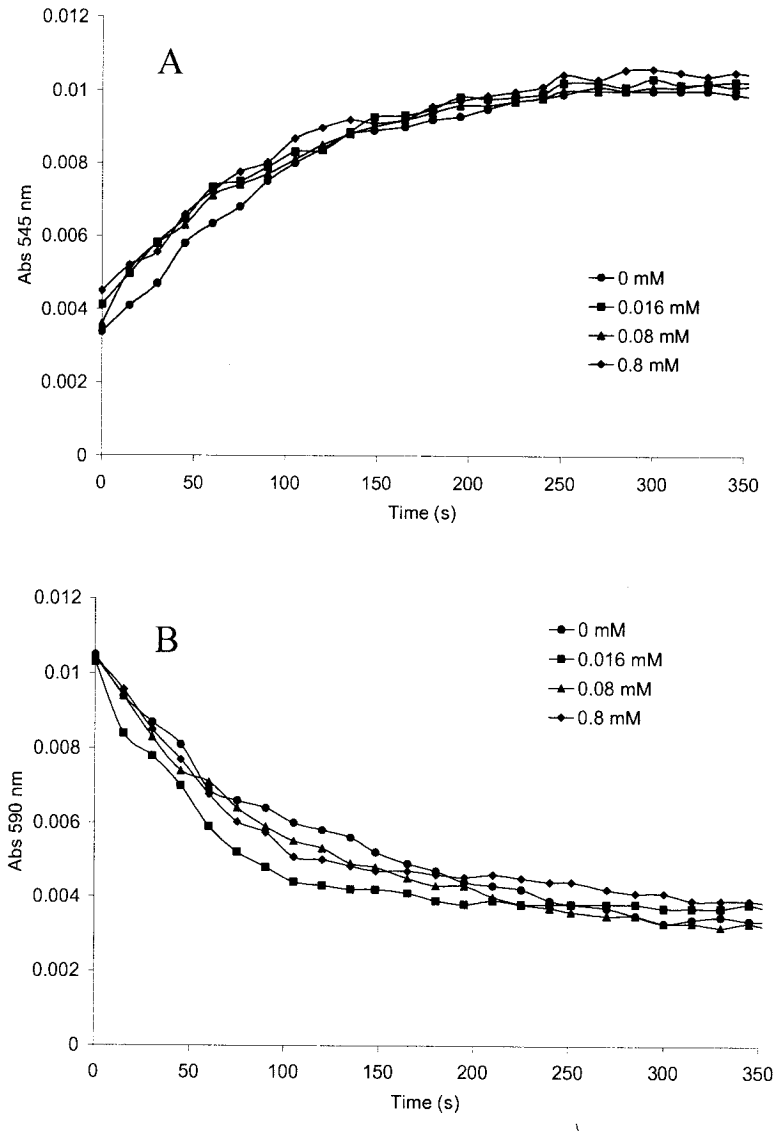


**Figure 2.9 Time course of the absorbance change at 545 and 590 nm during incubation of 0.299 mM SNAP and 0.297 mM GSH in the presence of $ZnAc_2$.** Absorbance at 545 nm (A) and (B) 590 nm. Measurements were made in a 1-cm cuvette in Tris buffer (pH 7.4) after 20 min incubation at room temperature. The $ZnAc_2$ concentrations are given in the figures.

### 2.3.4 Effects of CuZnSOD

CuZnSOD catalyzes NO transfer between SNAP and GSH (Figure 2.10) or d-hCys (Figure 2.11). A plateau is reached in ~100 s in the presence of CuZnSOD for the reaction between SNAP and GSH but at closer to 200 s in the absence of CuZnSOD. The reaction between SNAP and d-hCys in the presence of CuZnSOD shows a similar profile to the SNAP/GSH reaction (Figures 2.11 B *vs* 2.10 B) but in the absence of CuZnSOD the d-hCys reaction appears to approach completion after 350 s since the 590-nm absorbance is < 0.001 (Figure 2.11 A). Addition of chelator inhibits CuZnSOD-catalyzed NO transfer. However, the SNAP/d-hCys reaction is inhibited to a lesser extent than the SNAP/GSH reaction since the latter exhibits less change over 350 s compared to the former (Figure 12.2 A *vs* B).

### 2.3.5 Amperometric determination of free NO in SNAP/GSH solutions

To probe the mechanism of NO transfer, free NO levels were monitored in the SNAP/GSH incubates under different conditions. The free NO levels were found to be in the range of 1-2 μM in solutions containing 0.5 mM SNAP only (Figure 2.13 B). Free NO was also detected in the presence of SNAP plus 0.1 mM DTPA or 0.1 mM neocuproine revealing that the chelators do not fully inhibit release of NO (Figure 2.13 C, D). The free NO levels in the SNAP/GSH solutions in the presence of DTPA or neocuproine are similar to those in SNAP solutions without GSH (Figure 2.13 B, C *vs* 2.14 B, C).

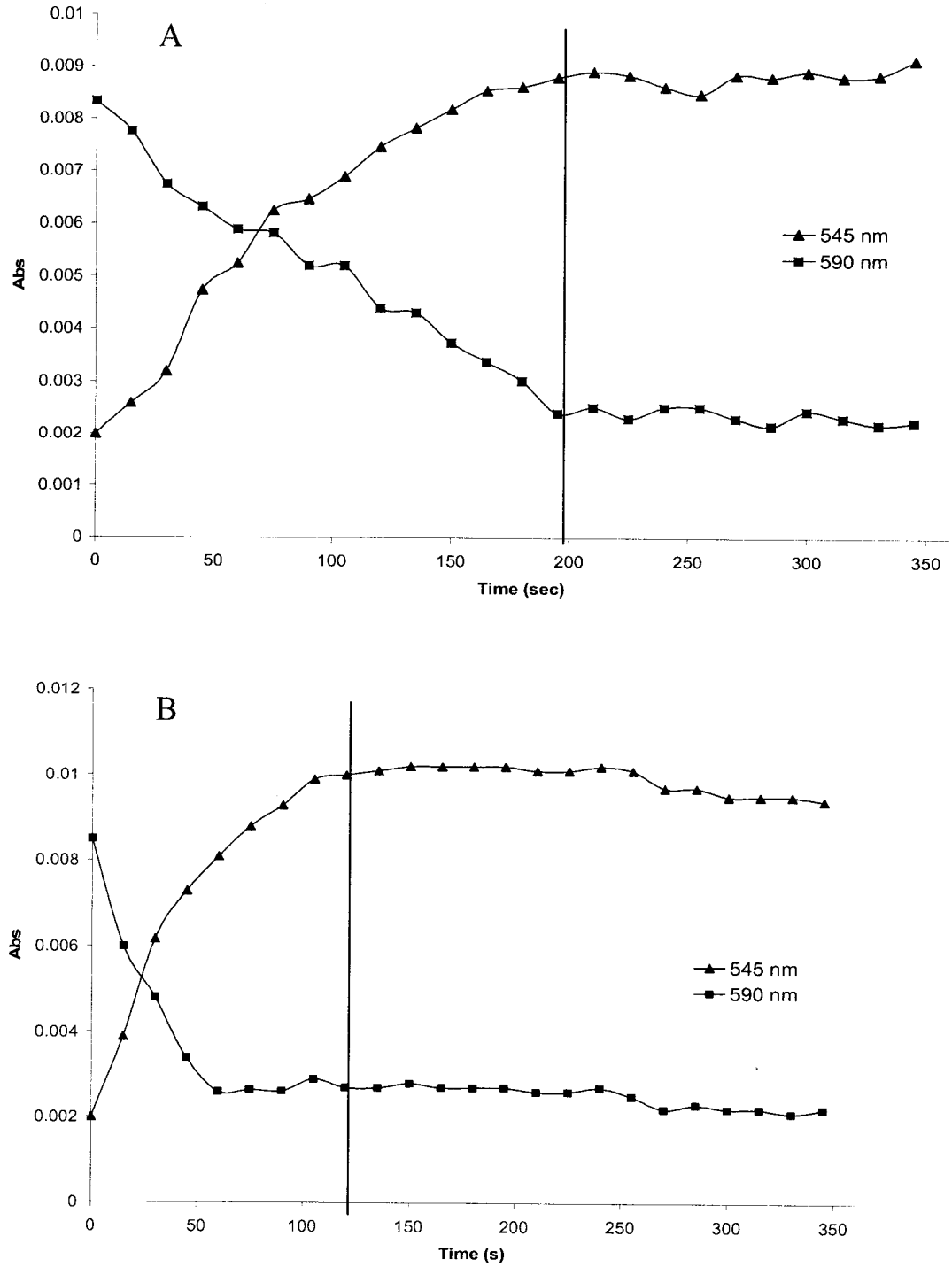


**Figure 2.10 Time course of the absorbance change during incubation of 0.299 mM SNAP and 0.297 mM GSH in the presence of CuZnSOD.** (A) Without CuZnSOD, and (B) with 8.3 μM CuZnSOD. The vertical lines represent the time at which the absorbance changes reach a plateau. No chelators were present. Absorbances were recorded in 10 mM Tris buffer (pH 7.4) in a 1-cm cuvette.

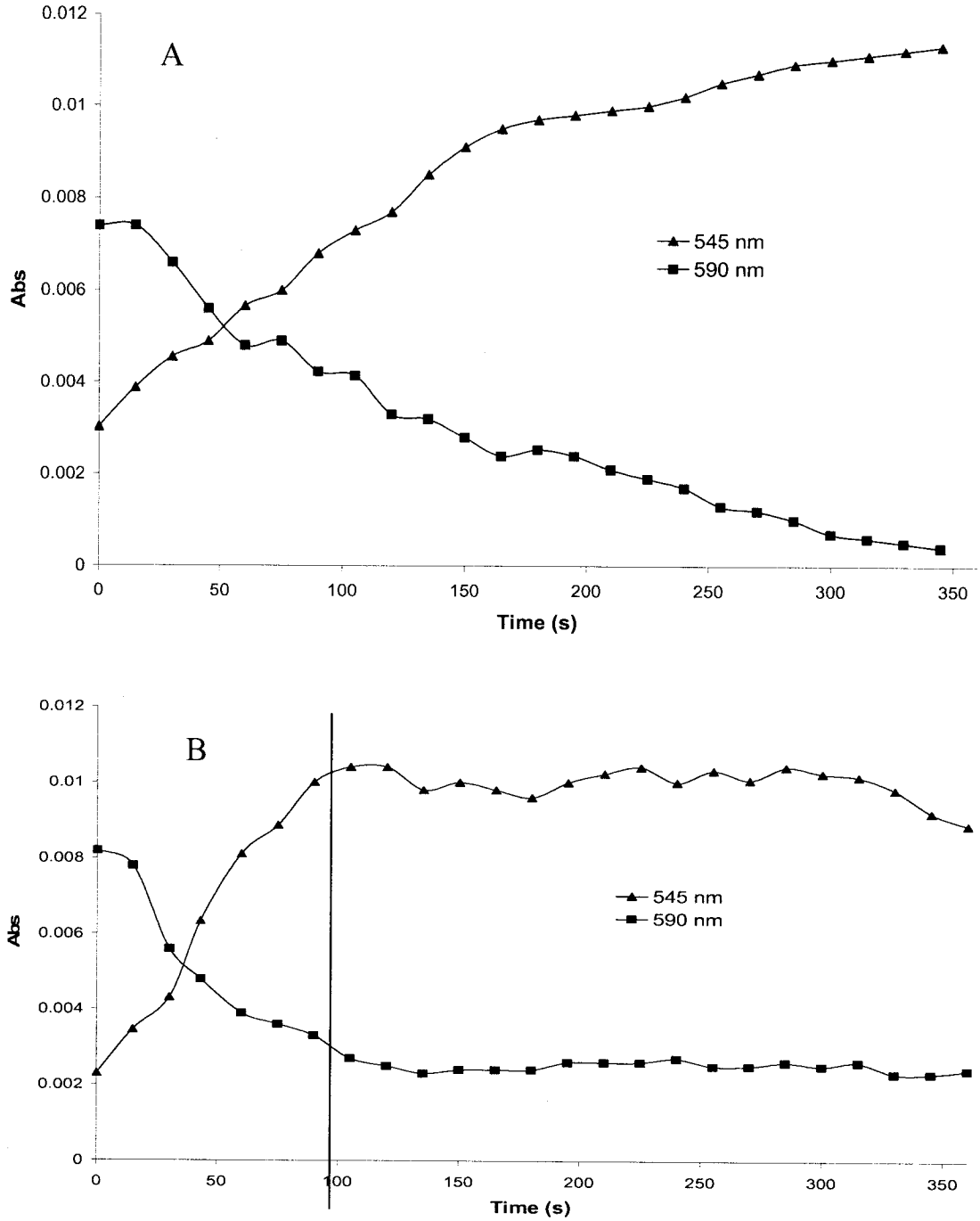


**Figure 2.11 Time course of absorbance change during incubation of 0.299 mM SNAP and 0.3 mM d-hCys in the presence of CuZnSOD.** (A) Without CuZnSOD and (B) with 8.3 μM CuZnSOD. The vertical lines represent the time at which the absorbance changes reach a plateau. No chelators were present. Absorbances were recorded in Tris buffer (pH 7.4) in a 1-cm cuvette.

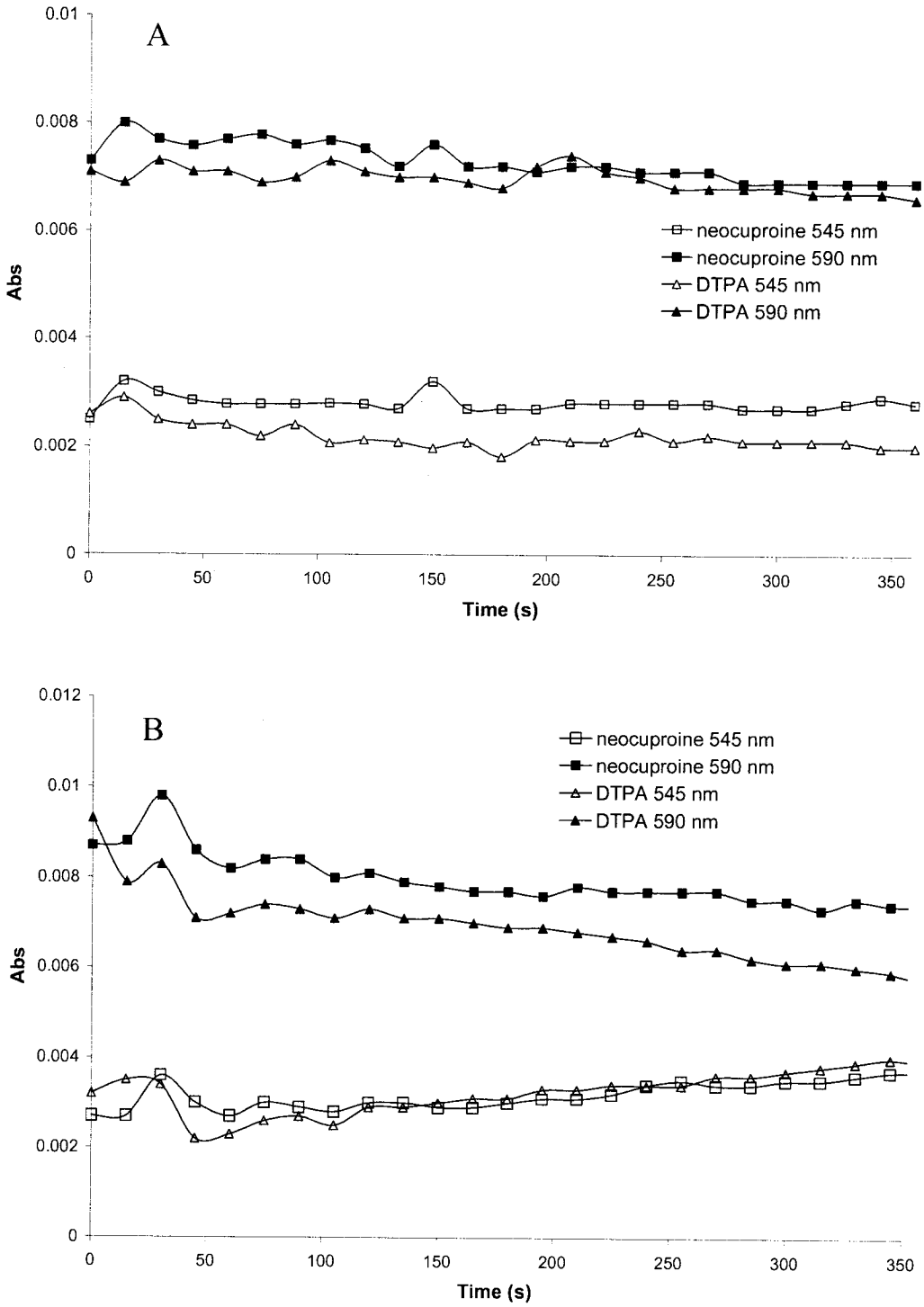


**Figure 2.12 Time course of the absorbance change time during incubation of 0.299 mM SNAP and primary thiol in the presence of 8.3 µM CuZnSOD + 0.1 mM DTPA or 0.1 mM neocuproine.** (A) 0.297 mM GSH and (B) 0.3 mM d-hCys. Absorbances were recorded in 0. 01 M Tris buffer (pH 7.4) in a 1-cm cuvette.

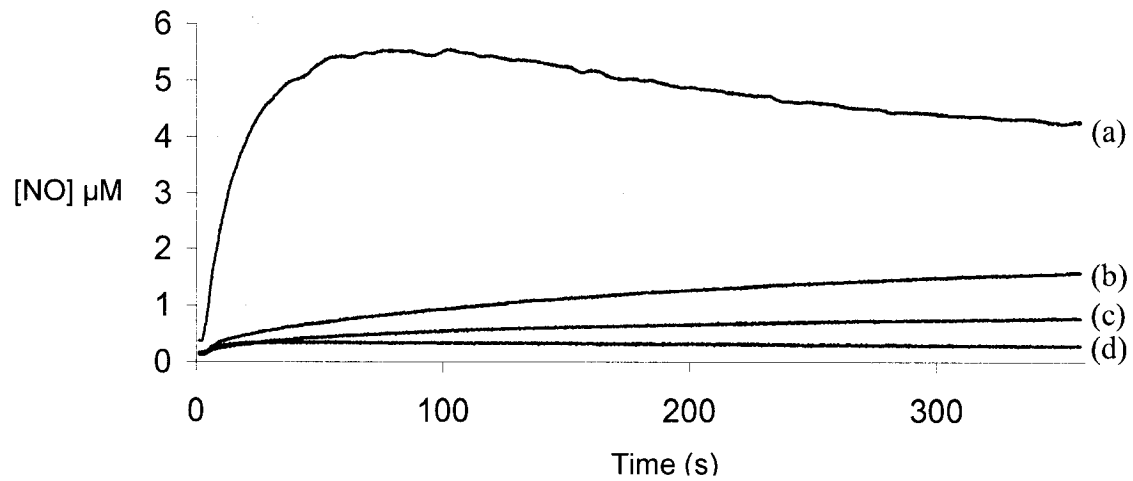


**Figure 2.13 Free NO concentration in 0.5 mM SNAP solutions in Tris buffer (pH 7.4) at room temperature.** (a) SNAP + 0.5 mM GSH, no chelator; (b) SNAP only, no chelator; (c) SNAP + 0.1 mM DTPA; (d) SNAP + 0.1 mM neocuproine. The NO concentration was determined using a NO-electrode in stirred air-saturated buffer in a 2-mL vial containing 600 μL of solution. SNAP was added at t=0 following 1-min equilibration of the electrode in the GSH or GSH + chelator solution

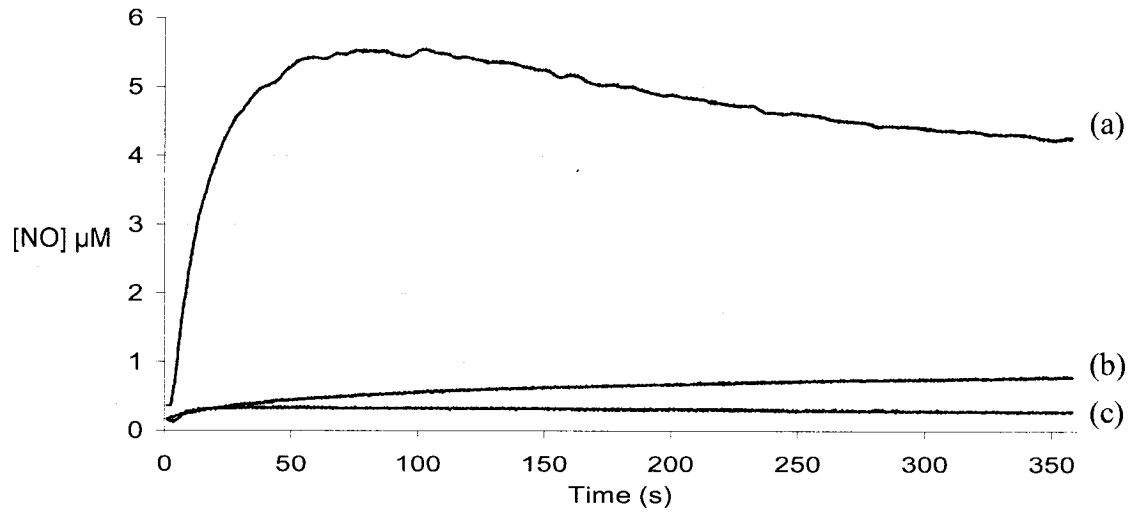


**Figure 2.14 Free NO concentration during incubation of 0.5 mM SNAP with 0.5 mM GSH in Tris buffer (pH 7.4) at room temperature**. (a) No chelators; (b) 0.1 mM DTPA; (c) 0.1 mM neocuproine. See legend of Figure 2.13 for experimental details.

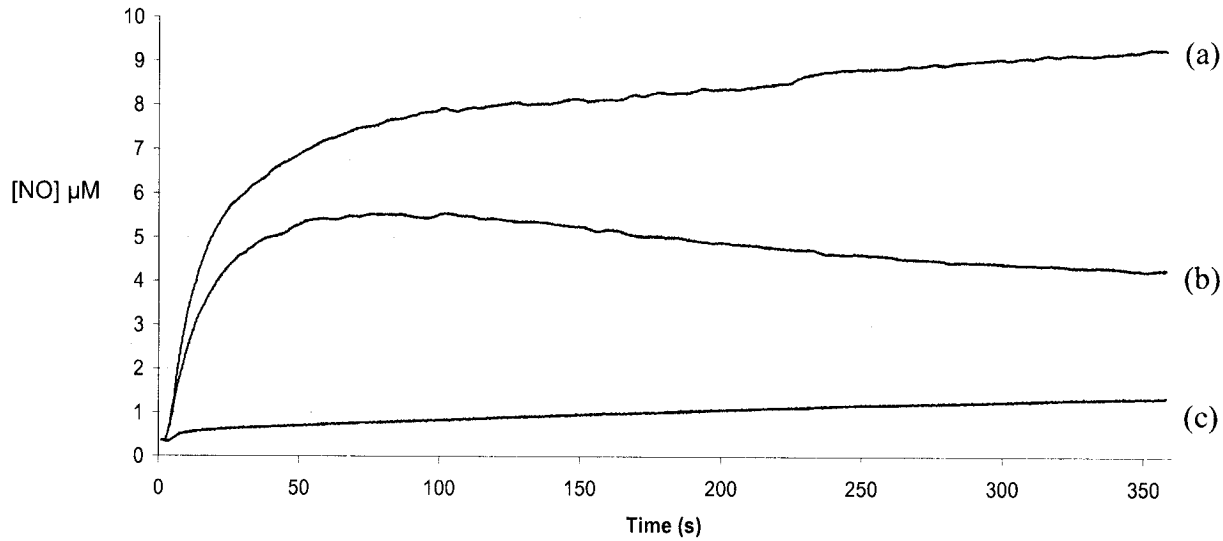


**Figure 2.15 Free NO concentration during incubation of 0.5 mM SNAP with 0.5 mM GSH in the presence of CuZnSOD.** (a) 5 μM CuZnSOD without chelator; (b) buffer without chelator; (c) 5 μM CuZnSOD + 0.1 mM DTPA. SNAP was added at t=0. See legend of Figure 2.13 for experimental details.

Addition of 5 μM CuZnSOD almost doubles the maximum free NO concentration measured in the SNAP/GSH incubate after 360 s (Figure 2.15). Since each CuZnSOD molecule contains 2 copper atoms, the bound-copper concentration is 10 μM. At this concentration, presumably copper-catalyzed decomposition of SNAP is the reason for this high free NO level.

# *Chapter 3 Dansyl homocysteine as a probe of NO transfer*

## 3.1 Introduction

The physical properties of dansyl homocysteine (d-hCys) have been reported as well as its synthesis (13). The relevant spectral properties of d-hCys and d-hCysNO were discussed in Section 1.3.

The two-step literature synthesis of d-hCysNO involves conversion of homocysteine (hCys) to hCysNO followed by dansylation (13). Gel purification yielded pure d-hCysNO. The critical part of the synthesis is the dansylation step, during which the amine moiety (the target for dansyl) should be deprotonated. This requires a pH > 9 (14) but it is well known that RSNOs exhibit low stability at high pH and form disulfides (39). Since it is difficult to separate RSNOs from RSSRs and minimal handling of RSNOs is desired, a new synthesis was developed here.

Using homocystine (h-$Cys_2$) as the starting material, dansylation was carried out in the first step followed by reduction of d-$hCys_2$ to d-hCys. The last step, which is performed just before use, is thiol nitrosation, to yield freshly prepared d-hCysNO (Figure 3.1). Using the disulfide as a starting compound, dansyl attack on the thiol is avoided. The overall d-hCysNO yield using our synthesis is ~ 40%.

## 3.2 Experimental

### 3.2.1 Preparation of d-$hCys_2$

Dansyl chloride is a electrophile that will attack the primary amino groups in $hCys_2$. Because the reactivity of secondary amines is lower than that of primary amines,

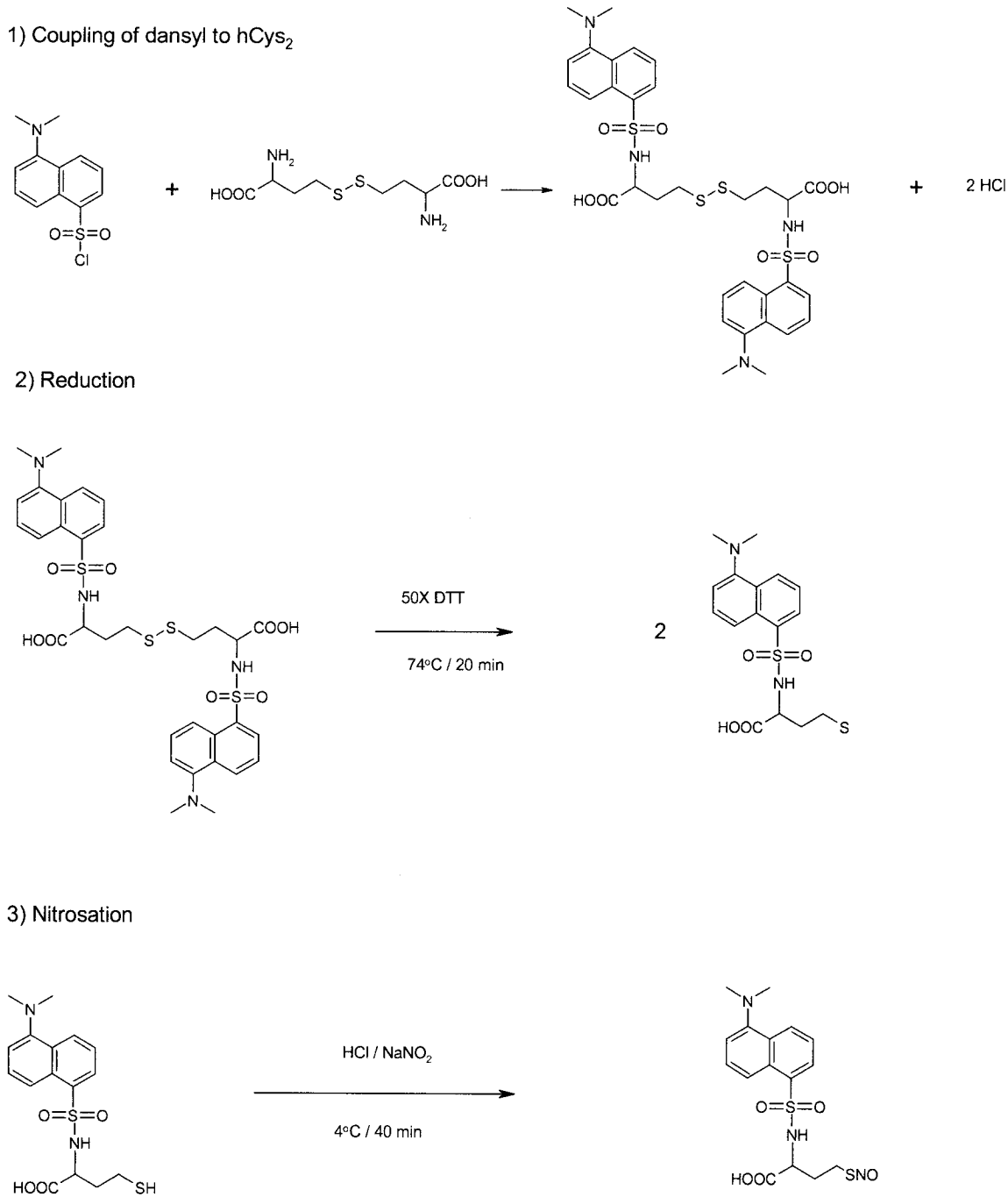


**Figure 3.1 Outline of the three-step synthesis of d-hCysNO developed in this thesis.** This procedure is a modification of the literature synthesis (25). DTT= dithiothreitol

the reaction will stop after one dansyl is attached to each amino group. In a side reaction, dansyl chloride hydrolyses to dansyl sulfonic acid, a fluorescent product with an emission

maximum at lower wavelength than d-$hCys_2$. Both reactions require high pH and at pH > 9.5 dansyl chloride hydrolysis is faster than its reaction with free amino groups. Both reactions release $H^+$, which lowers the buffer pH and at pH < 8 both reactions stop. The best buffer for dansyl labeling is a saturated borate solution with a pH of 9 (14).

Materials: Chemicals were obtained as follows: dansyl chloride, trifluoroacetic acid (TFA) from Sigma; sodium borate from ICN; acetone, acetonitrile, methanol, methylene chloride, ethyl acetate and HCl (all HPLC grade) from Fisher; 18.2 mΩ water from a Millipore Simplicity System; Chelex 100 from BioRad; pure NaOH from Fluka; silica gel from Silicycle and thin layer chromatograph (TLC) plates from Merck (Germany).

Procedures: Because traces of copper affect RSNOs stability, all glassware was soaked for 24 h in 1 M HCl, rinsed with 18.2 mΩ water and soaked for 24 h in water. To prepare the dansylation buffer, 40 g of sodium borate in 100 mL of water was stirred for 2 h. The precipitate was removed by filtration and the pH of the supernatant was adjusted to 7.0 with 12 M HCl. Trace metals were removed by adding 4 g of Chelex 100. The resin was removed by filtration, and the pH of the clear solution adjusted to pH 9.5 with pure NaOH. For the dansylation reaction 27 mg (0.1 mmol) of $hCys_2$ was dissolved in 30 mL borate buffer with 10 mL acetone. Dansyl chloride (80 mg; 0.3 mmol) was dissolved in 20 mL acetone and added dropwise with continuous stirring to the $hCys_2$ solution over 2 h at room temperature. The dansyl chloride/$hCys_2$ molar ratio was 3/1. The acetone was removed by evaporation by heating to 56°C and at this temperature, hydrolysis effectively consumed the excess dansyl chloride. The reaction mixture was allowed to cool down to room temperature and the pH was adjusted to 2.5 with concentrated HCl to

precipitate d-$hCys_2$. The precipitate was extracted in three 30-mL portions of ethyl acetate (24) and the dansyl sulfonate formed on dansyl chloride hydrolysis remained in the aqueous phase. HCl was extracted from the ethyl acetate solution with 200 mL of 18.2 mΩ water, and vacuum distillation was used to reduce the ethyl acetate volume to ~5 mL. The sample was fully dried on a Speed Vac (Model SC 1100, Savant) which yielded ~60 mg of yellowish solid that was stored at -80°C.

Purification of d-$hCys_2$ was carried out by silica gel column chromatography. Silica gel (40 g) was added to 100 mL of 5% methanol in methylene chloride (5%MeOH/$CH_2Cl_2$), poured into a 2.5x18-cm glass column, and washed with 100 mL of the same solvent. The yellow solid was dissolved in 0.5 mL 5% MeOH/$CH_2Cl_2$, added to the column, washed with 500 mL of 5% MeOH/$CH_2Cl_2$ and d-$hCys_2$ eluted with 20% MeOH/$CH_2Cl_2$. A hand-held UV lamp was used to locate the sample on the column. The solvent was reduced to 5 mL by vacuum distillation and the sample was dried on the Speed Vac to yield d-$hCys_2$ as a pale-yellow solid.

Electrospray ionization mass spectrometry (ESI-MS) confirmed the identity of the compound. The solid (0.5 mg) was dissolved in 50% acetonitrile/water and 0.05 % TFA. The solution was directly infused at a flow rate of 5 μmL/min into the ESI source of a Finnigan SSQ 7000 single qudrupole mass spectrometer. The capillary temperature was set to 250°C and the spray voltage at 4.5 kV. Product purity was verified by TLC. A solution of 0.5 mg product in 40 μL $CH_2Cl_2$ was prepared, a drop was applied using a glass capillary to a 3x10 – cm TLC plate, and 10%MeOH/$CH_2Cl_2$ was used as the mobile phase. The TLC plate was exposed to UV light to observe the fluorescent species.

### 3.2.2 Preparation of d-hCys

Materials: d-$hCys_2$ (Section 3.2.1), methanol, methylene chloride, dithiothreitol (DTT), silica gel; the suppliers are given in Section 3.2.1.

Procedures: d-$hCys_2$ 2.5 mg (2.7 μmol) was dissolved in 100 μL of 5%MeOH/$CH_2Cl_2$ and incubated with 21 mg (0.14 mmol) DTT for 20 min at 70°C in same solvent. The volume was adjusted to 500 μL with $CH_2Cl_2$ and DTT was removed by silica gel column chromatography as described in Section 3.2.1. The sample was added to the column, and a 300-mL wash of 5% MeOH/$CH_2Cl_2$ was sufficient to remove all DTT from the column. The d-hCys fraction was eluted with 20%MeOH/$CH_2Cl_2$ and the solvent was removed under nitrogen with gentle heating to ~ 40°C. The pale-yellow solid was analyzed by ESI-MS and TLC as described in Section 3.2.1, and stored at -80°C.

### 3.2.3. Preparation of d-hCysNO

Materials: d-hCys (Section 3.2.2), ultra pure HCl and ultra pure KOH from Fluka, ultra pure $NaNO_2$ from Sigma;

Procedures: d-hCys was S-nitrosated with close to 100% yield using a standard procedure (13). d-hCys (2 mg; 5 μmol) was disolved in 200 μL of 1 M HCl and cooled to 4°C in an ice bath. Equimolar $NaNO_2$ in 50 μL of $H_2O$ at 4°C was added in the dark with continuous stirring for 40 min. The pH was adjusted to 7.2 with KOH, and the d-hCysNO absorbance at 330 nm recorded on a Beckman DU-640 spectrophotometer.

### 3.2.4 Effects of SH modification on d-hCys fluorescence

S-nitrosation quenches d-hCys fluorescence due to intramolecular energy transfer between the dansyl donor and the S-NO acceptor (Figure 1.4). Fluorescence measurements on d-hCys and d-hCysNO were performed using the same sample concentration and the same instrument settings on an AMINCO-Bowman Series 2 luminescence spectrometer. The excitation slit was adjusted to 1 nm to allow minimum light to fall on the samples, and the emission slit was set to 4 nm. The PMT voltage was set using the default procedure on the Aminco. All experiments were performed at 25°C with freshly synthesized d-hCysNO (Section 3.2.3). Solutions of d-hCysNO were kept on ice for a maximum of 3 h before use.

The excitation and emission spectra of d-hCys and d-hCysNO were also recorded using same concentration for both compounds.

### 3.2.5 Fluorescence *vs* concentration; inner-filter effects

For quantitative analysis fluorescence intensity must vary linearly with fluorophore concentration. Due to sample absorption, the fluorescence is lower than expected at higher fluorophore concentrations. This apparent decrease in emission quantum yield is called the inner-filter effect. To establish the linear range of d-hCys fluorescence *vs* concentration samples containing different concentrations of the fluorophore (10 μM, 20 μM, 30 μM, 40 μM, 80 μM, 160 μM, 200 μM, 240 μM, 280 μM, 400 μM, 560 μM and 640 μM) were prepared. The fluorescence intensity was recorded using 380-nm excitation and 550-nm emission wavelengths. The same instrument settings were employed for all samples.

### 3.2.6 Effects of chelators on NO transfer from GSNO to d-hCys as monitored by fluorescence

Fluorescence changes in solutions containing 50 μM d-hCys and 50 μM GSNO were monitored over 600 s in the presence of different chelators. The excitation was set to 380 nm and the emission at 550 nm. The samples were prepared in 10 mM Tris buffer (pH 7.4) and 25 μM chelator (DTPA, DDC or neocuproine) was added where indicated. The d-hCys fluorescence in 600 μL buffer was recorded for 30 s before addition of GSNO in a minimum volume of buffer.

### 3.2.7 Analysis of products in SNAP/GSH incubates by mass spectrometry

ESI-MS was used to investigate the products formed on incubation of SNAP and d-hCys without any chelators. After 5 min incubation of 2 mM SNAP with 2 mM d-hCys in PBS (pH 7.4) at room temperature, a 10-μL aliquot was diluted to 1 mL with 50% acetonitrile/0.5% TFA and injected into the ESI source of the ThermoFinnigan SSQ 7000 mass spectrometer at a flow rate of 5 μL/min. The ESI source temperature was 180°C and the spray voltage 4.0 kV. The scanning range was m/z 300-750 and 20 spectra were averaged.

## 3.3 Results

### 3.3.1 Preparation of d-hCys$_2$

Dansyl chloride is insoluble in water so if no acetone was added to the buffer, the reaction was very slow. After 2 h, acetone was removed by evaporation from the mixture to allow extraction of d-hCys$_2$ with ethyl acetate. A pale-yellow precipitate of d-hCys$_2$ was formed on decreasing the pH to 2. If the volume of ethyl acetate was higher than 120 mL, the amount of HCl that dissolved in the acetate decomposed d-hCys$_2$ during solvent evaporation forming a blue-greenish precipitate.

d-hCys$_2$ bound to the silica-gel column equilibrated with 5%MeOH/$CH_2Cl_2$ was eluted with 20%MeOH/$CH_2Cl_2$. After removing the solvent, ~ 50 mg (66% yield) of pure solid d-hCys$_2$ was obtained. The molecular weight of d-hCys$_2$ is 734 and its ESI mass spectrum shows two peaks at m/z 368.2 and 735.3 corresponding to the $MH_2^{2+}$ and $MH^+$ ions, respectively (Figure 3.2). No ion corresponding to dansyl sulfonate (m/z 252), a side product of dansyl chloride hydrolysis (Section 3.2.1), is seen in Figure 3.2. Using a hand-held UV lamp, only a single fluorescent spot was observed on the TLC plate confirming the absence of dansyl sulfonate.

### 3.3.2 Preparation of d-hCys

The progress of d-hCys$_2$ reduction by DTT was monitored by TLC (Figure 3.3). If reduction was incomplete a second fluorescent spot due to d-hCys$_2$ was present (Figure 3.3 b). Traces of d-hCys$_2$ in the sample after reduction were removed by column chromatography as described in Section 3.3.1.

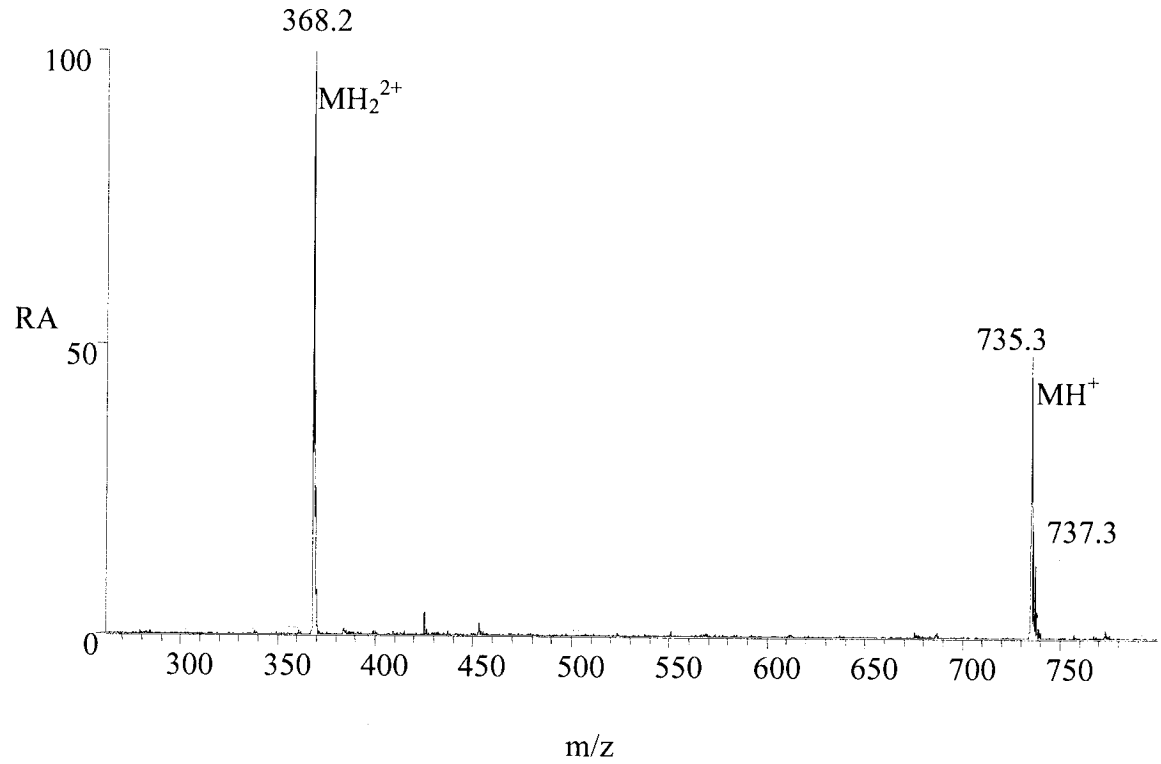


**Figure 3.2 ESI mass spectrum of d-hCys$_2$ in 50% acetonitrile/0.05% TFA.** The sample was infused directly into the ESI source at a flow rate of 5 μL/min. The source temperature was 250°C and the spray voltage 4.5 kV. The d-hCys$_2$ concentration was 17.6 μM. RA = relative abundance

d-hCys was eluted from the column before the disulfide, d-hCys$_2$. The progress of d-hCys$_2$ reduction was followed by TLC (Figure 3.3). Following removal of the solvent as described in Section 3.2.2, ~30 mg (40 % yield) of pale yellow solid was obtained. The ESI mass spectrum of purified d-hCys revealed only one peak at m/z 369.2. The low abundance peak at m/z 391.3 is bis(2-ethyl-hexyl)phthalate, which is present as an impurity in acetonitrile (Figure 3.4).

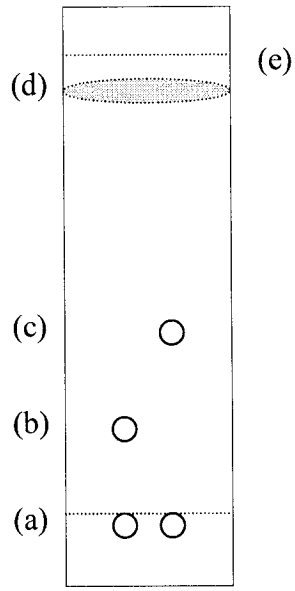


**Figure 3.3 Monitoring d-hCys$_2$ reduction by TLC.** (a) Application line; (b) d-hCys$_2$ spot; (c) d-hCys spot; (d) DTT spot; and (e) solvent front after 8 min. A 15-μL aliquot of the products from the reaction of 0.1 mM d-hCys$_2$ with 50-fold excess DTT was spotted on a 3x10-cm silica TLC plate and the products were separated using 20%MeOH/$CH_2Cl_2$. Spreading of DTT on the slide is due to the large concentration used.

### 3.3.3 Preparation of d-hCysNO

The SNO group of primary RSNOs exhibits an absorption maximum at 330 nm with ε~1000 $M^{-1}cm^{-1}$ (8). The calculated yield for d-hCysNO from d-hCys was ~95% using ε=1000 $M^{-1}cm^{-1}$. The high yield is consistent with literature data for acidic nitrosation of thiols (13).

### 3.3.4 Effects of SH modification on d-hCys$_2$ fluorescence

With the emission set to 554 nm, the excitation spectrum of d-hCys$_2$ exhibits a maximum at 330 nm. Because the SNO group absorbs at ~330 nm, an excitation

wavelength of 380 nm was used in all experiments to avoid inner-filter effects and to reduce photolysis. Once converted to the RSNO, the emission intensity of d-hCysNO decreased 11-fold (Figure 3.6).

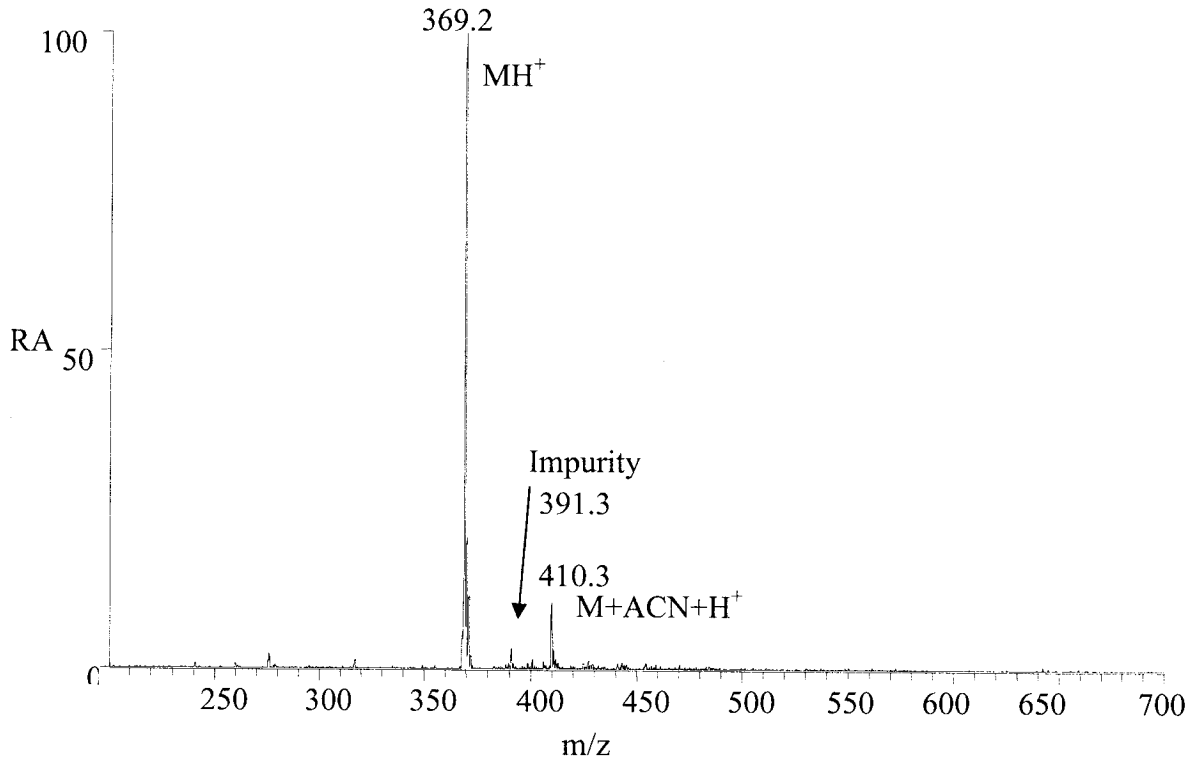


**Figure 3.4 ESI mass spectrum of d-hCys in 50% acetonitrile/0.05% TFA.** 10 μM d-hCys was injected into the ESI source at a flow rate of 5 μL/min. The source temperature was 250°C and voltage 4.5 kV. The low abundance peak at m/z 391.3 is bis(2-ethyl-hexyl)phthalate, which is present as an impurity in acetonitrile. RA= relative abundance

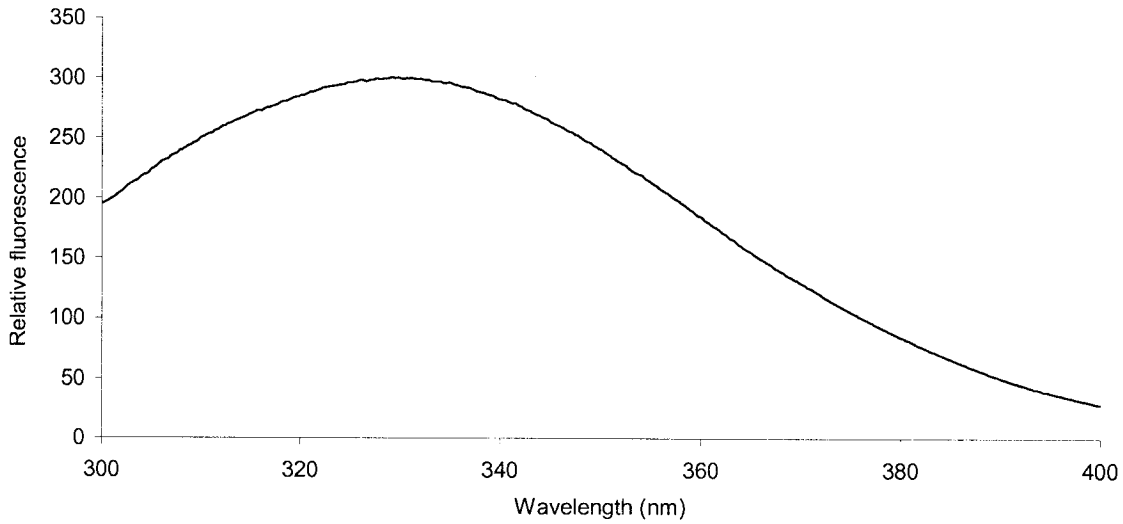


**Figure 3.5 Excitation spectrum of d-hCys with emission set to 550 nm.** 50 μM d-hCys was dissolved in PBS (pH 7.4), in a 1-cm quartz cuvette. The excitation and emission slits were 1 nm and 4 nm, respectively.

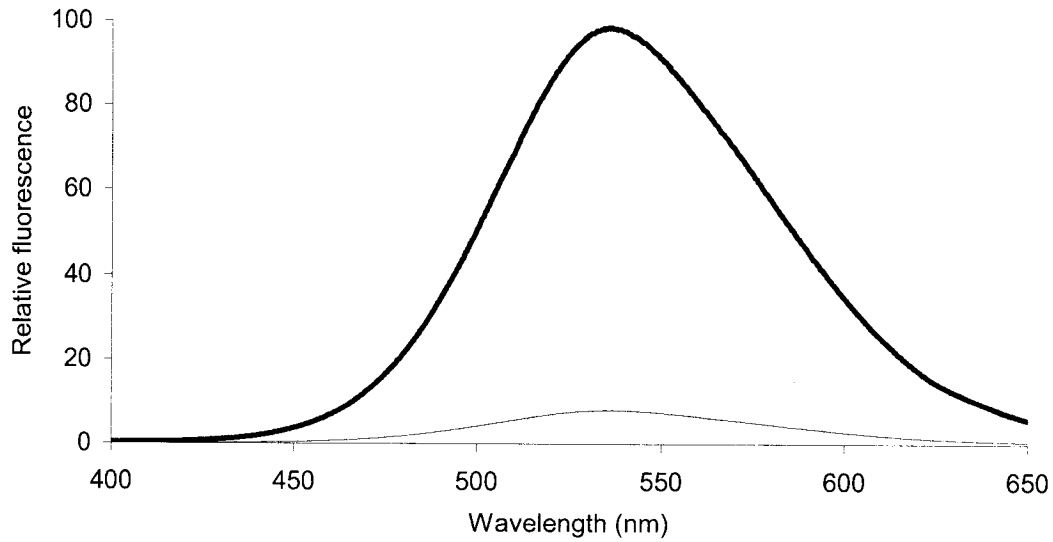


**Figure 3.6 Emission spectra of d-hCys and d-hCysNO on excitation at 380 nm.** Bold line, 50 μM d-hCys and thin line, 50 μM d-hCysNO. The experiment details are given in the legend of Figure 3.5

### 3.3.5 Fluorescence *vs* concentration; inner-filter effects

The plot of d-hCys$_2$ fluorescence *vs* concentration is linear in the region 0-150 μM (Figure 3.7). The instrumental parameters were set using 600 μM d-hCys$_2$, and all readings were made with the same settings of the PMT, and emission and excitation slits. The fluorescence samples containing <150 μM d-hCys$_2$ can be used for quantitative measurements. Since d-hCys$_2$ and d-hCys have similar absorption and emission profiles, the fluorescence of the thiol should be linear up to ~ 300 μM.

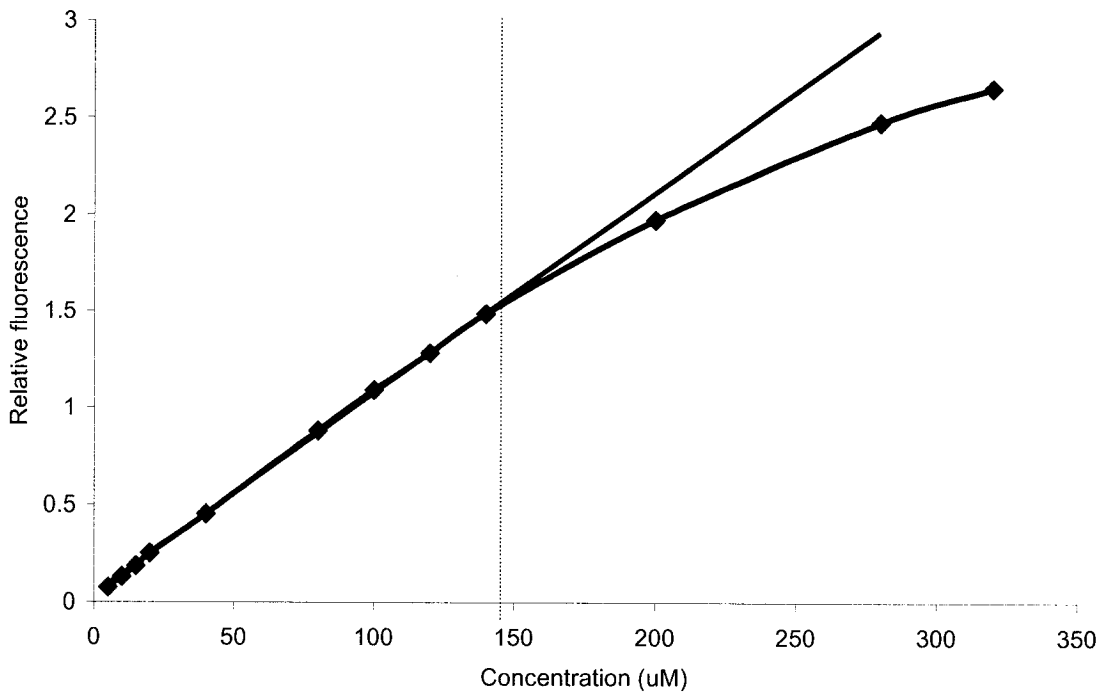


**Figure 3.7 Fluorescence *vs* concentration of d-hCys$_2$ in Tris buffer (pH 7.4) at room temperature.** Excitation, 380 nm; emission 550 nm; 1-nm excitation slit and 4-nm emission slit. The vertical dotted line indicates the limit of linearity. Deviations from linearity at high concentration are due to inner-filter effects.

### 3.3.6 Effects of chelators on NO transfer from GSNO to d-hCys as monitored by fluorescence

Following mixing of GSNO and d-hCys the NO moiety is partially transferred to the thiol and d-hCysNO is formed. The formation of d-hCysNO was detected by loss of sample fluorescence since S-nitrosation of d-hCys is accompanied by fluorescence quenching (Figure 3.6). On mixing GSNO and d-hCys in the absence of chelators ~ 50% of the latter is S-nitrosated (Figure 3.8).

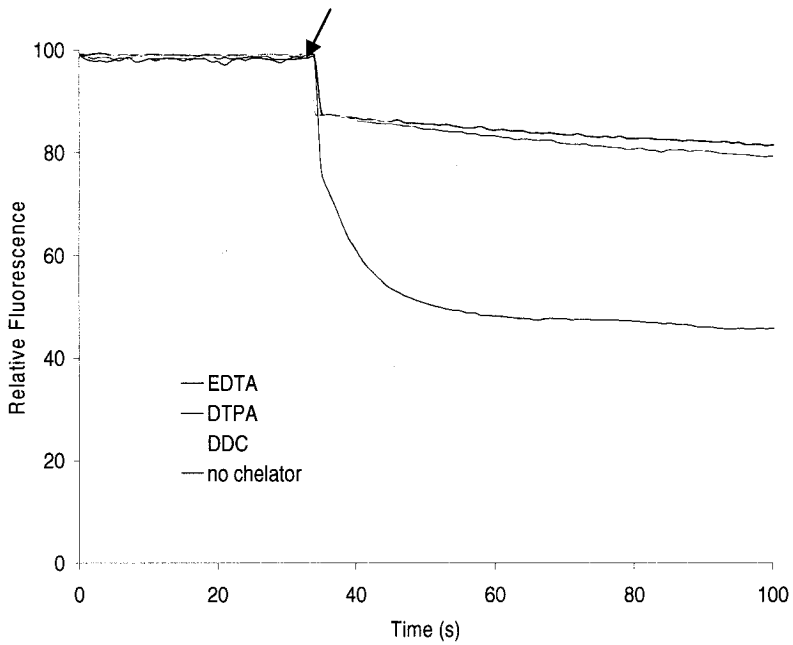


**Figure 3.8 Time course over 100 s of fluorescence variation following addition (at the arrow) of 50 μM GSNO to 50 μM d-hCys in the presence of chelators**. Where indicated, 25 μM chelator was present. The experimental conditions are given in legend of Figure 3.7.

In the presence of a $Cu^{2+}$ chelator (EDTA, DTPA, or DDC) the quenching is decreased, indicating that less d-hCysNO is generated. The rapid drop in fluorescence at the arrow is due to the inner-filter effect of GSNO, which absorbs at the excitation and emission wavelengths. The additional quenching in the absence of chelators indicates that copper-

catalyzed NO transfer is occurring and d-hCysNO is formed. However, the relief of quenching at longer times reveals that the d-hCysNO formed is slowly denitrosated (Figure 3.9).

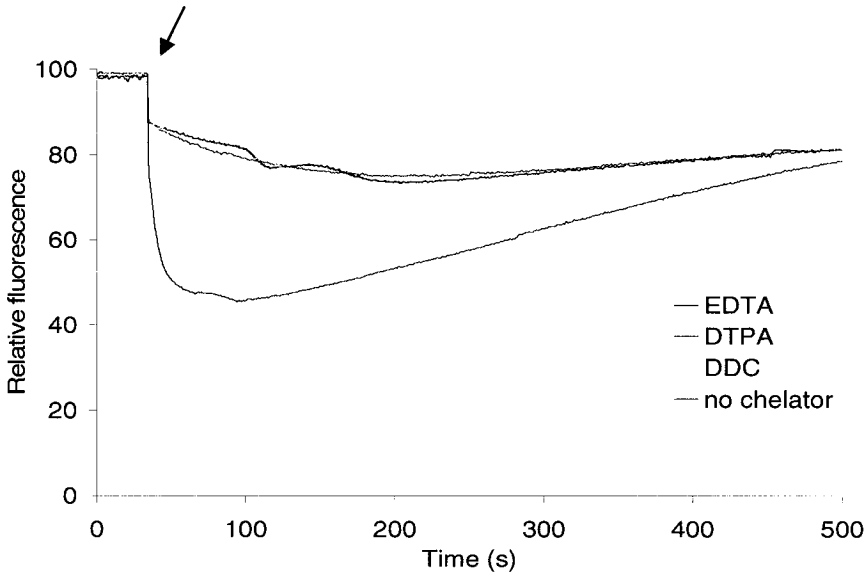


**Figure 3.9 Time course over 500 s of fluorescence variation following addition (at the arrow) of 50 µM GSNO to 50 µM d-hCys in the presence of chelators.** Where indicated, 25 µM chelator was present. The experimental conditions are given in legend of Figure 3.7

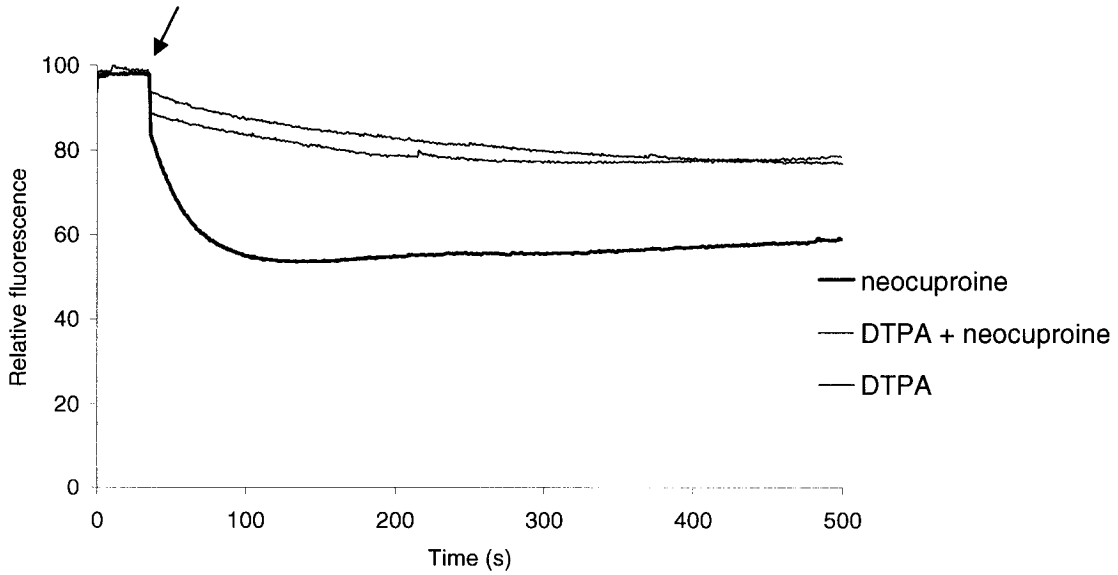


**Figure 3.10 Time course over 500 s of fluorescence variation following addition (at the arrow) of 50 µM GSNO to 50 µM d-hCys in the presence of 25 µM neocuproine.** The experimental conditions are given in legend of Figure 3.7

The large fluorescence quenching seen on neocuproine addition (Figure 3.10) is unexpected but reproducible. The drop in intensity is not due to an inner-filter effect of neocuproine since this is already present in the d-hCys solution. Further studies are necessary to probe the effect of neocuproine on the d-hCys/GSNO fluorescence profiles. Importantly, neoucproine did not have any unexpected effect on the absorption properties of the SNAP incubates (Figures 2.5 and 2.6).

### 3.3.7 Analysis of products from the GSNO/d-hCys incubate by mass spectrometry

After 5 min incubation of 2 mM GSNO with 2 mM d-hCys in PBS (pH 7.4) at room temperature, the mass spectrum of the products contains more species (Figure 3.11) than expected from direct $NO^+$ transfer between the reagents:

$$\text{GSNO} + \text{d-hCys} \rightleftharpoons \text{GSH} + \text{d-hCysNO} \qquad (3.1)$$

The most abundant peak at m/z 337.2 is identified as the $MH^+$ ion of GSNO and its $MNa^+$ ion appears at m/z 358.9. The second most abundant peak is at m/z 398.0 corresponding to d-hCysNO. The peak at m/z 369.2 corresponds to $MH^+$ of d-hCys but negligible ion intensity was observed at m/z 308 for $GSH_2^+$. Due to the low source temperature, acetonitrile adducts $(MH+41)^+$ of d-hCys (m/z 409.8) and d-hCysNO (m/z 439) are also observed.

GSSG ions expected at m/z 307 ($MH_2^{2+}$) and 613 ($MH^+$) are absent. The peak at m/z 673.3 was assigned to $MH^+$ of the mixed disulfide, d-hCys-SG, and the peak at m/z 736.4 to $MH^+$ of d-$hCys_2$. The low relative abundance of the disulfide peaks *vs* the RSNO and free thiol peaks is consistent with direct $NO^+$ transfer from GSNO to d-hCys since

disulfide formation in the ESI source due to the high capillary temperature (180°C) and high needle voltage (4 kV) cannot be excluded. However, the absence of significant ion intensity due to GSH is unexpected if reaction 3.1 is the dominant pathway of d-hCysNO formation.

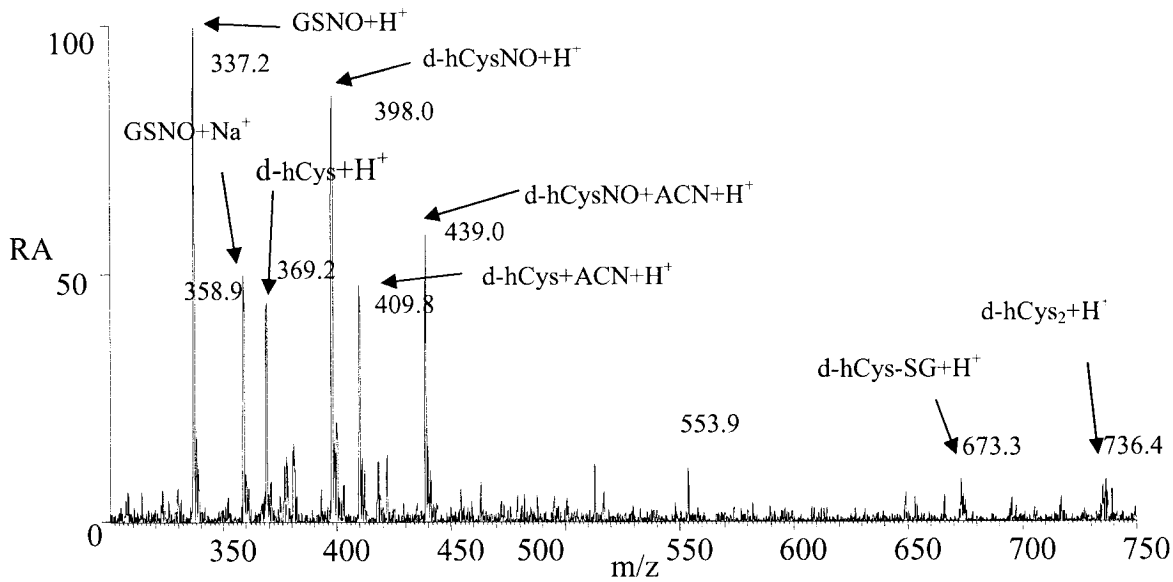


**Figure 3.11 Product ESI mass spectrum after 5 min incubation of 2 mM GSNO with 2 mM d-hCys in PBS (pH 7.4) at room temperature**. A 5-μL aliquot of the reaction mixture was diluted 100-fold into 50% acetonitrile/0.05% TFA and injected into ESI source at a flow of 5 μL/min. The source temperature 180°C and voltage 4 kV. No chelators were present.

# *Chapter 4 Effects of added copper on d-hCysNO stability*

## 4.1 Introduction

The catalysis by copper of NO release from RSNO is well known (22). The purpose of the experiments described in this chapter was to investigate the effects of added hydrated copper and of CuZnSOD on RSNO stability. Copper was added as $Cu^{1+}$, $Cu^{2+}$ and CuZnSOD. The RSNO used here was d-hCysNO, which becomes 10-fold more fluorescent on NO release (Figure 3.6). Thus, d-hCysNO is an excellent probe of NO transfer (Chapter 3). Sample fluorescence was recorded on an AMINCO-Bowman Series 2 Luminescence Spectrometer. The instrument settings were same as used in Section 3.2.4.

## 4.2 Experimental

Materials: d-hCysNO was prepared as described in Chapter 3. CuCl, $CuSO_4$ neocuproine, DTPA, and ascorbate were purchased from Sigma, and CuZnSOD from Roche. Tris buffer (10 mM, pH 7.4) was used in all experiments instead of PBS due to precipitation of the copper salts in the phosphate buffer. All glassware was cleaned to remove trace copper as previously described in Section 3.2.1. CuZnSOD was used without any purification.

### 4.2.1 Effects of added $Cu^{1+}$

Saturated CuCl in Tris buffer (pH 7.4) was prepared just before use because $Cu^{1+}$ undergoes aerobic oxidation to $Cu^{2+}$. The stock solution was replaced with a freshly prepared one after 20 min. CuCl solubility at 25°C is 6.2 mg/L corresponding to 60 μM

$Cu^{1+}$. A saturated CuCl solution was prepared by adding 2-3 mg of CuCl to 2 mL of Tris buffer (pH 7.4) in a centrifuge tube, which was centrifuged for 15 s at 10000 g, and the supernatant was used for the experiments.

The fluorescence spectra of 50 μM d-$hCys_2$ (the expected decomposition product; reactions 1.12 and 1.13) and of 100 μM d-hCysNO (reactant) in Tris buffer (pH 7.4) were used as controls. Saturated CuCl in 10 mM Tris buffer (pH 7.4) (300 μL) was added to the following samples in the same buffer: (1) 300 μL of 200 μM d-hCysNO without chelators; (2) 300 μL of 200 μM d-hCysNO plus 1 mM neocuproine; (3) 300 μL of 200 μM d-hCysNO plus 1 mM DTPA, and (4) 300 μL of 200 μM d-hCysNO plus 1 mM DTPA and 1 mM neocuproine. Fluorescence measurements were made after 20 min incubation of the reagents in the dark at room temperature. To investigate the time course of d-hCysNO decomposition, the fluorescence intensity was measured after 5, 15, 25 and 35 min incubation with $Cu^{1+}$.

### 4.2.2 Effects of added $Cu^{2+}$

$CuSO_4$ was used as a source of $Cu^{2+}$. A solution of 100 μM $CuSO_4$ in 10 mM Tris buffer (pH 7.4) were used as a stock, and 300 μL was added to samples 1-3 (Section 4.2.1), and to (5) 300 μL of 200 μM d-hCysNO plus 100 μM ascorbate; (6) 300 μL of 200 μM d-hCysNO plus 100 μM ascorbate and 1 mM neocuproine; (7) 300 μL of 200 μM d-hCysNO plus 100 μM ascorbate and 1 mM DTPA; and (8) 300 μL of 200 μM d-hCysNO plus 100 μM ascorbate, 1 mM DTPA and 1 mM neocuproine. The fluorescence intensity was measured following incubation at room temperature in the dark as described in Section 4.2.1.

### 4.2.3 Effects of added CuZnSOD

CuZnSOD contains 2 copper ions per molecule. Previous measurements in our lab (17) indicated that the enzyme does not contain any free copper ions. The final enzyme concentration in the sample was 25 μM, corresponding to 50 μM bound $Cu^{2+}$, which was the concentration of the copper salts used. The fluorescence spectra of 50 μM d-$hCys_2$ and of 100 μM d-hCysNO in Tris buffer (pH 7.4) was used as controls. To examine d-hCysNO decomposition in the presence of CuZnSOD, 300 μL of 50 μM CuZnSOD in Tris buffer (pH 7.4) was added to samples 1-4, Section 4.2.1. The fluorescence readings were recorded after 20 min incubation at room temperature in the dark.

## 4. 3 Results

### 4. 3.1 Effects of added $Cu^{1+}$

The fluorescence intensity of 50 μM d-$hCys_2$ at 550 nm was taken as 100 % (Figure 1, column 1) and the other intensities are relative to this value. The sample containing only 100 μM d-hCysNO exhibited the lowest fluorescence (15%; Figure 4.1, column 2). When $Cu^{1+}$ was added to d-hCysNO in the absence of chelators, the fluorescence increased to 87% (Figure 4.1, column 3) indicating the loss of NO from d-hCysNO. When chelators were present, either neocuproine or DTPA or both, the sample fluorescence remained low, close to the value for d-hCysNO only (Figure 4.1, columns 4, 5, 6). Samples 4 and 5 with neocuproine and DTPA, respectively, show similar intensities, indicating that both chelators are effective in inhibiting $Cu^{1+}$-catalyzed d-hCysNO decomposition.

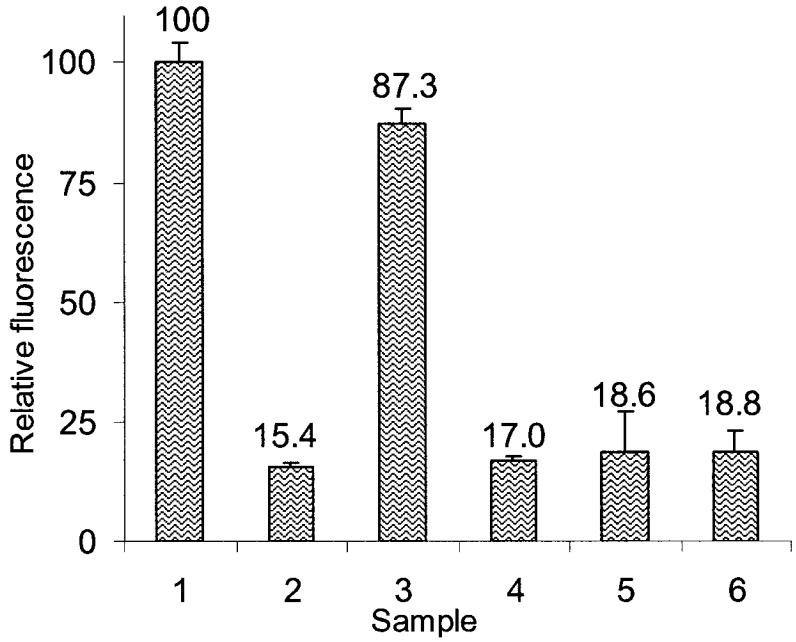


**Figure 4.1 Effects of added CuCl on the fluorescence of d-hCysNO solutions after 20 min incubation in the dark at room temperature.** (1) 50 μM d-$hCys_2$ without $Cu^{1+}$, (2) 100 μM d-hCysNO without $Cu^{1+}$, (3) 100 μM d-hCysNO + 30 μM CuCl, (4) 100 μM d-hCysNO + 30 μM CuCl + 500 μM neocuproine, (5) 100 μM d-hCysNO + 30 μM CuCl + 500 μM DTPA, (6) 100 μM d-hCysNO + 30 μM CuCl + 500 μM neocuproine + 500 μM DTPA. All samples were in 10 mM Tris buffer (pH 7.4). Following excitation at 380 nm, the emission intensity at 550 nm was recorded using excitation and emission slits of 1 nm and 4 nm, respectively. Each measurement was made in triplicate.

The time course of d-hCysNO decomposition following $Cu^{1+}$ addition indicates that in the first 5 min of incubation the fluorescence increases from ~15% to 81%. (Figure 4.2, columns 2, 3) followed by a slow increase from 81% to 96% during the next 30 min.

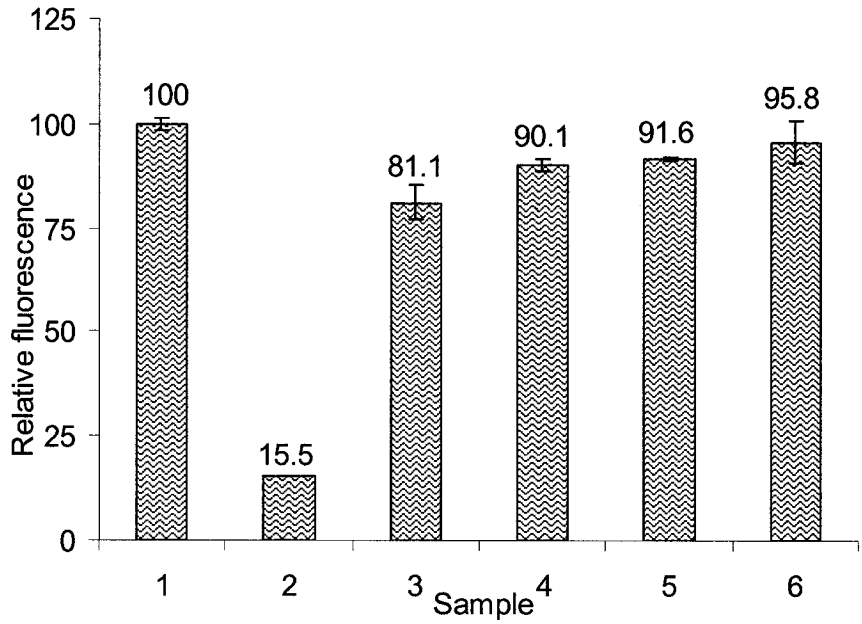


**Figure 4.2 Time course of the fluorescence change of a 100 μM d-hCysNO solution following addition of CuCl.** (1) 50 μM d-$hCys_2$ without $Cu^{1+}$, (2) 100 μM d-hCysNO without $Cu^{1+}$, 100 μM d-hCysNO (3) 5 min, (4) 15 min, (5) 25 min, and (6) 35 min after addition of 30 μM CuCl. The experimental conditions are given in the legend of Figure 4.1. Each measurement was made in triplicate.

### 4.3.2 Effects of added $Cu^{2+}$

As in the previous section, the fluorescence intensity of 50 μM d-$hCys_2$ was considered as 100%, and the other intensities are reported relatively to this sample. Again, d-hCysNO was found to exhibit the lowest fluorescence intensity and once copper was added, the fluorescence increased and reached a value of ~85% (Figure 4.3). In the presence of DTPA or neocuproine, the relative fluorescence was ~20%, close to that of d-hCysNO alone. When ascorbate was added to reduce $Cu^{2+}$ to $Cu^{1+}$, the intensity increased from ~ 85% to 98% in the absence of chelators (Figure 4.3, column 3 *vs* 6), and ~ 16% to 29% in the presence of the chelators (Figure 4.3, columns 4, 5 *vs* 7, 8). Interestingly, in

the presence of both chelators, the intensity remained low (16.4 %) even after ascorbate addition (Figure 4.3, column 9).

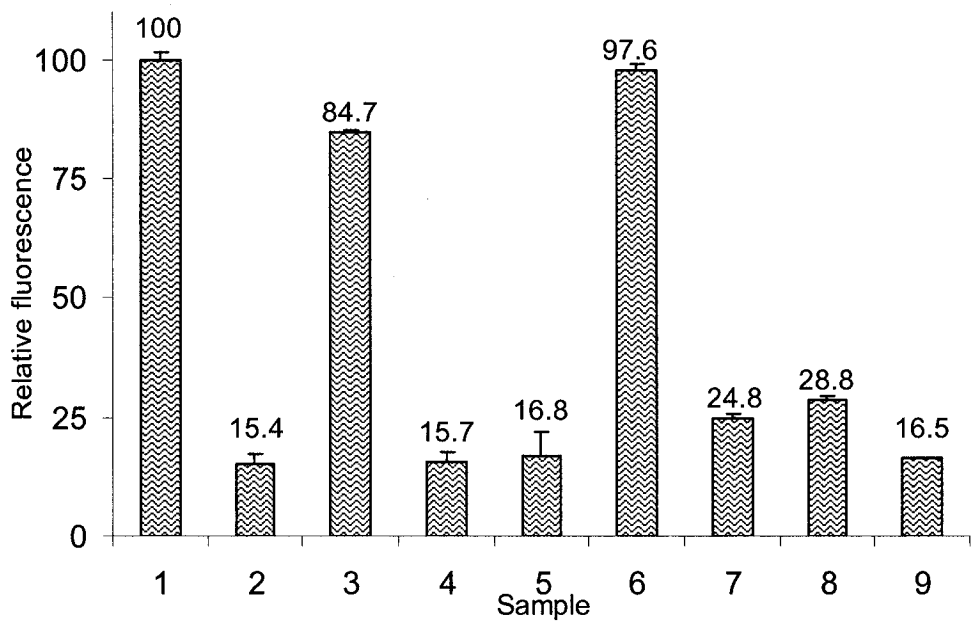


**Figure 4.3 Effects of added $CuSO_4$ on the fluorescence of d-hCysNO solutions** (1) 50 μM d-$hCys_2$ without $Cu^{2+}$, (2) 100 μM d-hCysNO without $Cu^{2+}$, (3) 100 μM d-hCysNO + 50 μM $CuSO_4$, (4) 100 μM d-hCysNO + 50 μM $CuSO_4$ + 500 μM neocuproine, (5) 100 μM d-hCysNO + 50 μM $CuSO_4$ + 500 μM DTPA, (6) 100 μM d-hCysNO + 50 μM $CuSO_4$ + 50 μM ascorbate, (7) 100 μM d-hCysNO + 50 μM $CuSO_4$ + 50 μM ascorbate + 500 μM neocuproine, (8) 100 μM d-hCysNO + 50 μM $CuSO_4$ + 50 μM ascorbate + 500 μM DTPA, (9) 100 μM d-hCysNO + 50 μM $CuSO_4$ + 50 μM ascorbate + 500 μM DTPA+ 500 μM neocuproine. Experimental conditions are given in the legend of Figure 4.1. Each measurement was made in triplicate.

### 4.3.3 Effects of added CuZnSOD

When CuZnSOD was added to d-hCysNO, the results (Figure 4.4) were similar to those obtained after adding CuCl or $CuSO_4$ (Figures 4.2 and 4.3). The relative fluorescence increased to 88% when the enzyme was present and the chelators inhibited the CuZnSOD-catalyzed increase in intensity (Figure 4.4). In the presence of either or

both chelators the fluorescence was in same range (~18±2%) indicating that both chelators are effective in inhibiting CuZnSOD catalysis.

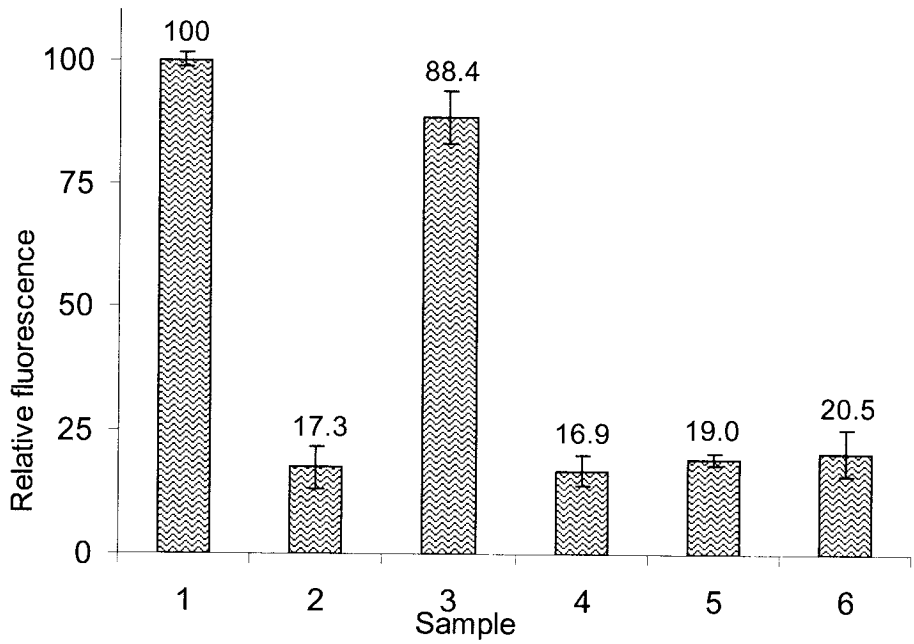


**Figure 4.4 Effects of added CuZnSOD on the fluorescence of d-hCysNO solutions.** (1) 50 μM d-$hCys_2$ without CuZnSOD , (2) 100 μM d-hCysNO without CuZnSOD, (3) 100 μM d-hCysNO + 25 μM CuZnSOD, (4) 100 μM d-hCysNO + 25 μM CuZnSOD + 500 μM neocuproine, (5) 100 μM d-hCysNO + 25 μM CuZnSOD + 500 μM DTPA, and (6) 100 μM d-hCysNO + 25 μM CuZnSOD + 500 μM DTPA + 500 μM neocuproine. Experimental conditions are given in the legend of Figure 4.1.

# *Chapter 5 Discussion*

## 5.1 Introduction

Fully understanding the biological role of NO requires fundamental knowledge of the mechanisms of NO-related reactions. The mechanism of NO transfer from RSNOs to low-molecular-weight thiols or protein thiols is still unknown. Studies on NO transfer from RSNOs to thiols have been reported previously (5, 6, 9) using different techniques including UV-vis absorption, HPLC, mass spectrometry (17, 18) and NO-selective-electrode measurements. The most popular method of study of the NO transfer/release reactions of RSNOs is absorption spectroscopy. This method's limitations arise from the fact that primary RSNOs have similar visible absorption profiles, making kinetic studies difficult to monitor. HPLC and mass spectrometry methods do not allow direct kinetic analysis. However, absorption spectroscopy can be used to carry out direct kinetic studies on NO-transfer reactions between tertiary RSNOs such SNAP and primary thiols.

Literature reports exist that d-hCys fluorescence is quenched upon conversion to d-hCysNO (13). No studies on NO release/transfer mechanisms were carried out using this compound. It has also been reported that the reaction products depend on the RSNO concentration (31). A sensitive method such as fluorescence allows use of low reactant concentrations so that reactions can be studied at close to *in vivo* conditions. In the present work, copper's role in NO transfer from GSNO to d-hCys was investigated as another model for *trans*-S-nitrosation between low-molecular-weight thiols.

Many reports (10) suggest that NO transfer between thiols is not affected by copper and that the metal is just involved in RSNO decomposition (15, 16). It is common

procedure to add copper chelators such as DTPA or neocuproine at a concentration of 50-100 μM when investigating RSNO reactions. Neocuproine is a well-known $Cu^{1+}$-specific chelator. Each copper coordinates two neocuproine ligands. The bonds to the tetracoordinated cuprous ion are disposed toward the apexes of a tetrahedron so that the planes of the two phenantroline molecules are at right angles to each other (30) (Figure 5.1). This stabilize the $Cu^{I}$ complex by increasing the reduction potential ($E°Cu^{II}/Cu^{I}$) from 0.15 V (35) to 0.594 V (36).

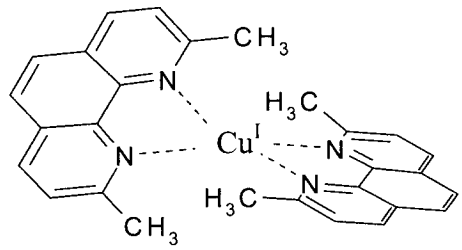


**Figure 5.1 $Cu^{I}$(neocuproine)$_2^{+}$ complex**

GSNO stability is concentration dependent (15). At concentrations >1 mM, GSSG generated by GSNO breakdown will be present in high enough concentration to chelate $Cu^{2+}$ and inhibit catalysis by redox turnover of copper.

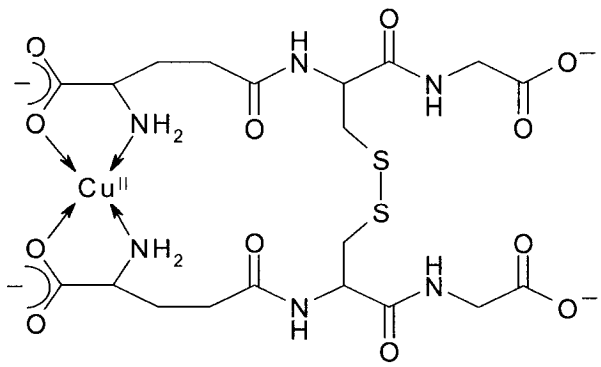


**Figure 5.2 $Cu^{II}(GSSG)^{2-}$ complex (22)**

A proposed $Cu^{II}(GSSG)^{2-}$ complex (Figure 5.2) has been published (22). To avoid copper chelation by GSSG, (GSX (X=H, NO) concentrations less than 1 mM was used for all reactants except the incubation of 3 mM SNAP with 3 mM GSH in presence of 1 mM DTPA (Figure 2.2).

Recently, our lab demonstrated that trace copper catalyzes NO transfer from RSNOs to proteins thiols (17, 18). The effect of copper on NO transfer between low-molecular-weight RSNOs and thiols was investigated here. A mechanism for NO transfer is proposed below. The time course of the visible absorbance changes during the reaction of the tertiary RSNO, SNAP, with GSH and d-hCys and the fluorescence changes during the reaction of GSNO with d-hCys were investigated.

The free copper levels were altered using different copper chelators. Since copper is present in small concentrations in distilled water (17), inductively coupled-plasma mass spectrometry (ICP-MS) was used in our lab to accurately measure copper levels in water from a Millipore simplicity system. The results show the presence of ~1 μM copper in all samples (17), which is enough to catalyze RSNOs breakdown. In Chapter 4, the effects of copper, added as either a cuprous (CuCl) or cupric ($Cu\ SO_4$) salt, on RSNO stability were investigated by exploiting the fluorescence properties of d-hCysNO. Likewise, the effects of added CuZnSOD were examinated since our lab has reported that this enzyme efficiently catalyzes NO transfer between GSNO and protein thiols (16,17).

## 5.2 NO transfer from SNAP to GSH

The reaction between SNAP and primary thiols, in particular GSH, is well known. Many studies have investigated different aspects of this reaction including the effects of pH and the kinetics (19, 20). The characteristic absorption band of primary RSNOs at 545

nm is red-shifted to 590 nm in SNAP. This difference allows NO transfer between primary and tertiary thiols to be directly probed using visible absorption spectroscopy (Figure 5.3).

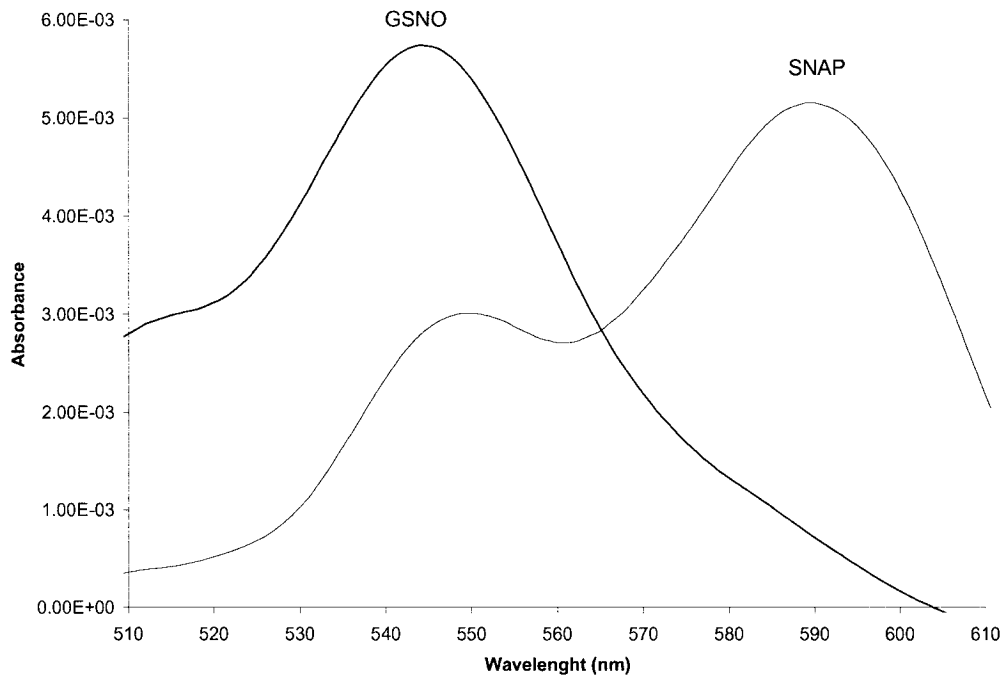


**Figure 5.3 Visible absorption spectra of GSNO and SNAP.** 0.3 mM GSNO (bold line) and 0.3 mM SNAP in 10 mM Tris buffer (pH 7.4) in a 1-cm cell at room temperature

Following mixing of SNAP and GSH, the intensity of the 590-nm absorption decreased and a new absorption peak appeared at 545 nm (Figure 2.2). This indicated that the SNAP concentration decreased and GSNO increased due to reaction 5.1:

$$\text{SNAP} + \text{GSH} \rightleftharpoons \text{NAP} + \text{GSNO} \quad (5.1)$$

Many authors propose direct $NO^+$ transfer from SNAP to GSH without metal-ion catalysis (15, 16). This proposal cannot fully explain our results. NO transfer upon SNAP

incubation with equimolar GSH slows down ~20-fold in the presence of 50 μM chelator (Figure 2.5). The difference in reaction rate in the presence and absence of copper chelators provides strong evidence that copper plays a role in NO transfer. In the presence of 1 mM DTPA, after 60 min both SNAP and GSNO were present at equilibrium as determined by visible absorption (Figure 2.2). In the reaction without chelators, SNAP was completely consumed within 2 min, and the GSNO absorption at 545 nm indicated that 0.297 mM GSH was converted to 0.296 mM GSNO (Table 5.2 and Figure 2.4).

These results suggest, as in the protein reactions, that trace copper plays an important role in NO transfer from RSNOs to low-molecular-weight thiols (17, 18). If the mechanism is similar to that proposed for copper-catalyzed decomposition of RSNOs (eqs 1.11 and 1.12), NO transfer from SNAP to GSH will occur as follows:

$$Cu^{2+} + GS^- \rightleftharpoons Cu^{1+} + GS^\bullet \quad (5.2)$$

$$Cu^{1+} + SNAP \rightleftharpoons Cu^{2+} + NAP^- + NO^\bullet \quad (5.3)$$

$$GS^\bullet + NO^\bullet \rightleftharpoons GSNO \quad (5.4)$$

$$GS^\bullet + GS^\bullet \rightleftharpoons GSSG \quad (5.5)$$

In this scheme, GSNO formation (eq 5.4) must compete with GSSG formation (eq 5.5). If the NO acceptor is a protein thiyl radical, the probability of disulfide bond formation upon copper reduction should be low due to steric constraints. However, for low-molecular-weight thiols, thiyl radical dimerization is reported to be rapid (10).

An isobestic point, or a point at which the level of absorption remains unchanged as a reaction proceeds, requires stoichiometric interconversion of the absorbing species. The presence of a point approaching an isosbestic point during the SNAP/GSH reaction (Figures 2.2 and 2.4) indicates that NO transfer from SNAP to GSH is close to 100% efficient in the presence or absence of DTPA and that the NO released from SNAP does not partake in any side reactions. If NO is quantitatively transferred from SNAP to GSH then the sum of the SNAP + GSNO concentrations should equal the starting concentration of SNAP (1.997 mM) at all times. Tables 5.1 and 5.2 summarize the RSNO concentration obtained at different times during the reaction by fitting the absorbance between 520 and 620 nm to a sum of the individual RSNO absorbances. The results in the Table 5.1 reveal that in presence of 1 mM DTPA, at equilibrium the mixture contains ~ 45% GSNO and 55% SNAP. In the absence of chelators, the SNAP concentration at equilibrium is 0.001 mM and the GSNO is 0.296 mM (Table 5.2). An attempt to monitor the reverse reaction (**GSNO+NAP→GSH+SNAP**) failed due to the low solubility of NAP in aqueous solutions. At 0.3 mM NAP the solution was cloudy.

The calculated differences between the starting SNAP concentration and the total RSNO concentration at any time during the reaction ($\Delta conc_t$, Tables 5.1 and 5.2) are an average of 0.048 ± 0.027 mM in the presence of chelators and 0.009 ± 0.027 mM in the absence of chelators. Since $\Delta conc_t$ varies randomly with time rather than growing with time, these values must represent experimental errors and not the amount of SNAP taking part in side reactions. Hence, it is assumed that conversion of SNAP to GSNO took place in both incubates with no GSSG formation (eq 5.5).

**Table 5.1 SNAP and GSNO concentrations in 1 mM DTPA solution *vs* time**

| Time (min) | [SNAP] (mM) | [GSNO] (mM) | $\Delta conc_t$ (mM)[b] |
|---|---|---|---|
| 0 | 1.997 | 0.000 | 0.000 |
| 10 | 1.769 | 0.228 | 0.003 |
| 15 | 1.623 | 0.363 | 0.014 |
| 20 | 1.511 | 0.467 | 0.022 |
| 25 | 1.385 | 0.558 | 0.057 |
| 30 | 1.243 | 0.680 | 0.077 |
| 35 | 1.127 | 0.784 | 0.089 |
| 40 | 1.020 | 0.923 | 0.057 |
| 45 | 0.966 | 0.982 | 0.052 |
| 50 | 0.923 | 1.026 | 0.051 |
| 55 | 0.873 | 1.071 | 0.056 |

a) For reaction conditions see legend of Figure 2.2

b) $\Delta conc_t = [SNAP]_0 - ([SNAP]_t + [GSNO]_t)$

**Table 5.2 SNAP and GSNO concentrations *vs* time in an incubate without chelators**

| Time (s) | [SNAP] (mM) | [GSNO] (mM) | $\Delta conc_t$ (mM)[b] |
|---|---|---|---|
| 0 | 0.299 | 0.000 | 0.000 |
| 15 | 0.210 | 0.078 | 0.001 |
| 30 | 0.172 | 0.117 | 0.011 |
| 45 | 0.103 | 0.160 | 0.037 |
| 60 | 0.070 | 0.224 | 0.006 |
| 90 | 0.034 | 0.254 | 0.012 |
| 105 | 0.024 | 0.269 | 0.007 |
| 120 | 0.013 | 0.283 | 0.004 |
| 135 | 0.011 | 0.291 | 0.008 |
| 150 | 0.005 | 0.287 | 0.008 |
| 165 | 0.003 | 0.290 | 0.007 |
| 180 | 0.002 | 0.296 | 0.002 |

a) For reaction conditions see legend of Figure 2.4

b) $\Delta conc_t = [SNAP]_0 - ([SNAP]_t + [GSNO]_t)$

In the presence of 1 mM DTPA without GSH, there is no decrease of absorbance at 590 nm over 60 min (Figure 2.3). Thus, SNAP photolysis (eq 5.6) does not play a role in NO transfer.

$$\text{SNAP} \overset{h\nu}{\rightleftharpoons} \text{NO}^{\bullet} + \text{NAP}^{\bullet} \qquad (5.6)$$

The reaction of SNAP with GSH in the presence of 1 mM DTPA is a slow process and takes ~60 min to reach equilibrium (Figure 2.2). The results are in agreements with those published (19). The minimum amount of DTPA necessary to inhibit the copper–catalyzed NO transfer is in the range of 2-5 μM. DTPA at the higher concentration of 5 μM completely inhibits copper catalysis but not at 2.5 μM (Figure 2.7). Combined with previous ICP-MS measurements that revealed a concentration of 1 μM copper in our lab water (17), these results suggest that other metal species are competing with copper for the chelator or that $K_D$ for the $Cu^{II}(DTPA)^{3-}$ complex is ~2 μM. The latter seems unlikely since the $K_D$ for $Cu(EDTA)^{2-}$ is $< 10^{-18}$ (35).

GSSG is a weaker copper chelating agent than DTPA since 25 μM GSSG only partially inhibits copper-catalyzed NO transfer. In fact, 40 μM GSSG was required to fully inhibit the copper-catalyzed reaction (Figure 2.8). Since 25 μM GSSG inhibits copper catalysis by ~50% (Figure 2.8), it can be assumed that ~50% of the free copper is bound to the chelator at this concentration. Thus, the $K_D$ of the $Cu^{II}(GSSG)^{2-}$ complex (Figure 5.2) must be ~25 μM.

## 5.3 d-hCys as a probe for NO transfer reactions

To determine whether the SNAP/GSH reaction is typical of NO-transfer reactions, a sensitive probe of S-nitrosation was synthesized. d-hCys (Figure 1.10) is a fluorescently labelled thiol that upon S-nitrosation (Figure 5.4) is only weakly fluorescent (Figure. 3.6) due to intramolecular energy transfer. Thus, the fluorescence decrease is correlated with the ratio of thiol to S-nitrosothiol conversion. Since fluorescence is a more sensitive probe than absorption, reagent concentrations in the NO-transfer reaction were decreased 4-fold from 0.2 mM to 50 μM. Both d-hCys and d-hCysNO were used as reagents. Fluorescence increases were monitored with d-hCysNO as a reactant, and fluorescence decreases were monitored with d-hCys as a reactant.

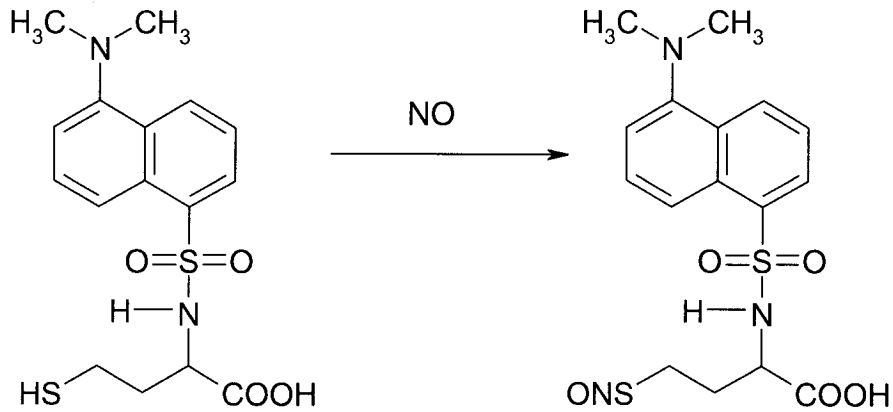


**Figure 5.4 d-hCys conversion to d-hCysNO**

The literature synthesis (25) was modified to prepare the d-hCys probe. The reaction buffer was changed from saturated carbonate buffer to saturated borate buffer, which has strong buffering capacity. The anhydrous $Na_2SO_4$ treatment of the ethyl acetate extract (25) was eliminated due to strong d-$hCys_2$ absorption by the salt with loss of

yield. DTT incubation to reduce d-hCys$_2$ to d-hCys was added. Any attempt to double the amount of reactants from for synthesis failed since d-hCys$_2$ decomposed to a blue precipitate during the longer solvent evaporation time. The advantage of the synthesis described in Chapter 3 is that pure d-hCys can be produced with a yield of ~ 40% and stored in the freezer. The simple treatment of the thiol with acidified $NaNO_2$ is sufficient to produce pure d-hCysNO in 30 min just before use with a yield of 98% (Figure 3.1).

The reaction of GSNO and d-hCys (Figure 3.8) exhibits similar kinetics as the reaction between SNAP and GSH (Figure 2.5). Bearing in mind that the initial drop in fluorescence on GSNO addition is due to an inner-filter effect (Section 3.3.6), the copper chelators dramatically decrease the NO transfer rate but do not stop it completely (Figure 3.8). The reaction without chelators exhibits minimum fluorescence in < 25 s followed by a gradual fluorescence increase between 100-500 s (Figure 3.9). In the presence of 25 μM copper chelator, the fluorescence decreased by only ~10% (*vs* ~50% in the absence of chelator) followed by a slow increase of fluorescence due to d-hCysNO denitrosation. The time necessary to reach the minimum fluorescence was ~170-200 s after GSNO addition in the presence of chelators *vs* < 25 s in the absence of chelators.

Significant fluorescence quenching and no increase in fluorescence due to denitrosation at longer times were observed in the sample with neocuproine (Figure 3.10). As discussed in Section 3.3.6, further study of the effect of neocuproine on d-hCys fluorescence in the presence of GSNO is necessary.

To confirm that the observed rapid fluorescence decrease in Figure 3.9 is due to the formation of d-hCysNO, the reaction mixture was analyzed by ESI-MS. The spectrum shows the presence of abundant $MH^+$ ions of d-hCysNO (m/z 389), d-hCys (m/z 369),

and GSNO (m/z 337) as well less abundant $MH^+$ ions of d-hCys-GS (m/z 673.3) and d-$hCys_2$ (m/z 736) (Figure 3.11). The presence of the disulfides may arise from processes in the ESI source due to the high voltage (4 kV) and high capillary temperature (180°C) required for efficient ion formation. GSSG was detected when pure GSNO was analyzed with the same instrument (data not show). However, copper-catalyzed GSNO cleavage in solution could also give the observed GSSG. The following reactions would give the products observed in Figure 3.11 in the absence of chelators:

$$Cu^{2+} + \text{d-hCys} \rightleftharpoons Cu^{1+} + \text{d-hCys}^{\bullet} \quad (5.7)$$

$$Cu^{1+} + \text{GSNO} \rightleftharpoons Cu^{2+} + NO^{\bullet} + GS^{-} \quad (5.8)$$

$$\text{d-hCys}^{\bullet} + NO^{\bullet} \rightleftharpoons \text{d-hCysNO} \quad (5.9)$$

$$\text{d-hCys}^{\bullet} + \text{d-hCys}^{\bullet} \rightleftharpoons \text{d-hCys}_2 \quad (5.10)$$

$$Cu^{2+} + GS^{-} \rightleftharpoons Cu^{1+} + GS^{\bullet} \quad (5.2)$$

$$GS^{\bullet} + \text{d-hCys}^{\bullet} \rightleftharpoons \text{d-hCys-GS} \quad (5.11)$$

$$GS^{\bullet} + GS^{\bullet} \rightleftharpoons GSSG \quad (5.5)$$

Thus, d-$hCys_2$ and d-hCys-GS can be formed by radical recombination reactions both in solution and in the ESI source (10). The latter arises from the homolysis of RSNO to $RS^{\cdot}$ and NO in the source. Interestingly, ions due to GST and GSSG were not detected in Figure 3.11. This implies that any $GS^{-}$ produced must be consumed by reaction 5.2 and that reaction 5.11 is faster than reaction 5.5. If a significant amount of GSNO is

converted to d-hCys-GS then the ionization efficiency of this species must be low because of the low relative abundance of its $MH^+$ ion (Figure 3.11).

## 5.4 Effects of $Zn^{2+}$ on NO transfer

The results in Chapter 3 show that copper plays a catalytic role in NO transfer. Both $Cu^{1+}$ and $Cu^{2+}$ chelators are effective inhibitors of copper catalysis indicating that redox turnover of copper is necessary. $Cu^{1+}$ catalyzes the reductive cleavage of the S-NO bond to give $RS^{\cdot}$ and $NO^{\cdot}$ (eq 5.8). In contrast, $Hg^{2+}$ effectively catalyzes heterolytic cleavage of the S-NO bond to give $RS^-$ and $NO^+$:

$$Hg^{2+} + RSNO \rightleftharpoons HgRS^+ + NO^+ \qquad (5.12)$$

$$NO^+ + HO^- \rightleftharpoons HONO \rightleftharpoons H^+ + NO_2^- \qquad (5.13)$$

Reactions 5.12 and 5.13 are the basis of the well-known Saville assay (7) for RSNO determination *via* $NO_2^-$ measurements. Nitrite is rapidly formed on $NO^+$ hydrolysis to nitrous acid HONO, which has a $pK_a$ of 3.15. $Zn^{2+}$ is unlikely to participate in redox reactions with thiols or RSNOs but the Lewis acid properties of $Zn^{2+}$ could promote cleavage of the S-NO bond like its group 12 congener, $Hg^{2+}$. Our results (Figure 2.9) show no influence of added $Zn^{2+}$ on NO transfer. Even 0.8 mM $Zn^{2+}$ had no effect on the RSNO/R'SH incubates (Figure 2.9) whereas 11 μM $Cu^{2+}$ was sufficient to completely cleave any RSNOs present. In conclusion, added $Zn^{2+}$ has no catalytic effect on NO transfer and its Lewis acidity is insufficient to promote cleavage of the S-NO bond.

## 5.5 Effects of added copper on d-hCysNO stability and on NO transfer reactions

Copper was added to d-hCysNO solutions and to incubates of RSNO and R'SH. The purpose of these experiments was to investigate the enhancement of the rate of d-hCysNO decomposition by added copper. Incubation of d-hCysNO with 30 μM $Cu^{1+}$ or $Cu^{2+}$ gave similar results. The fluorescence increase revealed denitrosation of d-hCysNO (Figures 4.1 and 4.3) and both DTPA and neocuproine inhibit copper-catalyzed d-hCysNO decomposition. This is strong evidence that redox turnover of the metal occurs during copper-catalyzed decomposition so that chelating either $Cu^{1+}$ or $Cu^{2+}$ inhibit catalysis (Figure 4.1, columns 4, 5, 6 and Figure 4.3, columns 4, 5). When ascorbate and $Cu^{2+}$ were added *vs* $Cu^{2+}$ alone the relative fluorescence (Figure 4.3, column 6 *vs* 3) was higher and essentially 100%. The reason for this is most likely the faster copper turnover in the presence of the reductant, ascorbate. From the data in Figures 4.1 to 4.3 it is clear that added copper strongly catalyses d-hCysNO breakdown. Sample 2 of each figure shows the fluorescence of d-hCysNO after 20-min incubation without chelators and without added copper. Under these conditions there is ~ 1 μM trace copper impurity. In the case of d-hCysNO, this level of copper is not an efficient catalyst of reductive denitrosation, which is consistent with the reported stability of hCysNO solutions compared to CysNO solutions (8). Copper-catalyzed d-hCysNO decomposition occurs mainly within the first 5 min of CuCl addition since the sample fluorescence is 81% after this period (Figure 4.2, columns 1, 2, 3).

Similar to the $Cu^{2+}$ and $Cu^{1+}$ salts, CuZnSOD also catalyzes d-hCysNO denitrosation (Figure 4.4). Likewise, addition of CuZnSOD to SNAP/d-hCys incubates

increased the rate of NO transfer since a plateau was reached in 95 s and 350 s with and without enzyme, respectively (Figure 2.11). Similar results were obtained when GSH was replaced by d-hCys where the absorbance changes reached a plateau in 105 s and 200 s in the presence and absence of CuZnSOD, respectively. The rate of CuZnSOD-catalyzed NO transfer from SNAP to d-hCys is faster than to GSH (Figure 2.12).

## 5.6 Use of d-hCysNO in a rapid screen for NO acceptors on proteins

The large fluorescence increase of d-hCysNO on denitrosation (Figure 3.6) can be used to rapidly screen for NO acceptors on proteins. The method is qualitative but yields results in less than 5 min and requires only a lamp to excitate the dansyl moiety. A 500-μL solution of 100 μM d-hCysNO and 100 μM protein were incubated in a centrifuge tube for 3 min. The same amount of d-hCysNO without protein was used as a control. A hand-held UV lamp was used to excite the dansyl fluorophore. Samples exhibiting higher fluorescence than the control are assumed to contain NO acceptors while those that exhibit the same fluorescence as the control do not contain NO acceptors.

In Figure 5.5, samples a-c contain 100 μM d-hCysNO with GSH, BSA and papain, respectively, whereas e-g contain 100 μM d-hCysNO only. The high fluorescence of samples a-c is consistent with the ability of GSH (Chapter 2), BSA (19) and papain (34) to participate in NO-transfer reactions. Samples g and h contain another danslyated RSNO, d-GSNO with and without BSA as a NO acceptor. Due to steric hindrance, intramolecular energy transfer in d-GSNO is less efficient than in d-hCysNO and the fluorescence quenching upon S-nitrosation is low. Thus d-GSNO was not explored here as a probe of NO-transfer reaction.

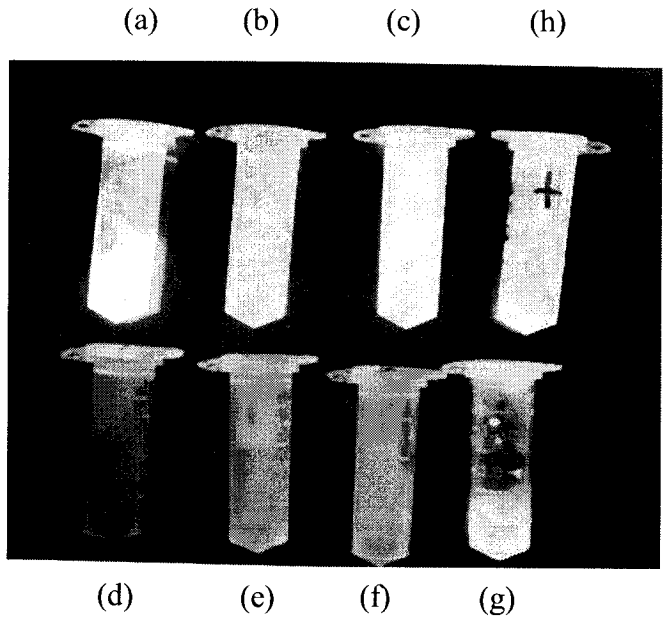


**Figure 5.5 Use of d-hCysNO in a fluorescence screen for NO acceptors.** (a-f) 100 μM d-hCysNO; (a) + 10 mM GSH, (b) + 50 μM BSA, (c) + 3 mM papain, (g-h) 100 μM d-GSNO; (h) + 50 μM BSA. All samples were in PBS (pH 7.4) with no chelators and were excited with a hand-held UV lamp.

Use of 100 μM d-hCysNO as a staining solution for BSA and papain in a native gel or membrane did not result in protein detection. Probably, the total amount of loaded protein (~5 μmol) was too low to produce a detectable increase in fluorescence above background due to d-hCyNO photolysis by the UV lamp.

## 5.7 Conclusions

### 5.7.1 Mechanism of copper-catalyzed NO transfer

Mayer *et al.* (29) reported the growth of a transient characterized by absorbance at 355 nm with a rate constant of $10^8$ $M^{-1}s^{-1}$ on mixing $Cu^{2+}$ with GSH. The authors assign this band to S-to-$Cu^{2+}$ charge transfer. The transient disappears in ~100 ms and a new

transient that absorbs below 320 nm is formed. The final product is a complex of $RS^-$ with $Cu^{1+}$ characterized by the presence of absorption at 265 and 295 nm. Thus, adding $Cu^{2+}$ to a thiol yields a complex containing $Cu^{1+}$ and the thiolate anion.

Combining the results of Mayer *et al.* (29) and the results of Chapters 2 and 3, the mechanism of NO transfer between low-molecular-weight thiols given by reactions 5.2-5.4 (or reactions 5.7-5.9) is modified as folows:

$$Cu^{2+} + RS^- \rightleftharpoons Cu^{II}(RS)^+ \rightleftharpoons Cu^{I}(RS^\cdot) \quad (5.14)$$

$$Cu^{I}(RS^\cdot) + R'SNO \rightleftharpoons Cu^{I}(RS^\cdot)(R'SNO) \quad (5.15)$$

$$Cu^{I}(RS^\cdot)(R'SNO) \rightleftharpoons Cu^{2+} + R'S^- + RSNO \quad (5.16)$$

The sum of eq 5.14-5.16 is:

$$R'SNO + RS^- \rightleftharpoons R'S^- + RSNO \quad (5.1)$$

In the first step (eq 5.14) the thiolate anion $RS^-$ binds to trace copper to yield a thiyl radical complex of $Cu^{1+}$. A mechanism is proposed by Meyer *et al.* (29) but the details of how $Cu^{2+}$ is reduced to $Cu^{1+}$ are unknown. The second step (eq 5.15) is the interaction of $Cu^{I}(RS^\cdot)$ with R'SNO, followed by intramolecular NO transfer generating the new S-nitrosothiol, RSNO, $Cu^{2+}$ and the new thiolate $R'S^-$ anion. For efficient NO transfer from R'SNO to RSH, $RS^-$ must be a better electron donor to $Cu^{2+}$ than $R'S^-$:

$$RS^- + Cu^{2+} \rightleftharpoons Cu^{I}(RS^\cdot)^+ \quad (5.17)$$

$$R'S^- + Cu^{2+} \rightleftharpoons Cu^{I}(R'S^\cdot)^+ \quad (5.18)$$

If reaction 5.17 is favored over 5.18 then the equilibrium in the reaction 5.1 will be pushed to the right and the products will be mainly RSNO and R'SH. This is observed for

copper-catalyzed NO transfer between SNAP and GSH (Figure 2.4), and CuZnSOD-catalyzed NO transfer between SNAP and d-hCys (Figure 2.11 A). Intramolecular NO transfer (eq 15) would explain the stoichiometric transfer of NO from SNAP to GSH seen in Figure 2.4 and Table 5.2 in the absence of metal chelators. Thus, conditions that favor binding of $RS^-$ and R'SNO to copper should promote efficient NO transfer. Nonetheless, the NO electrode measurements (Figures 2.13-2.15) reveal a steady–state concentration of ~5-10 μM free NO in the SNAP (0.5 mM)/GSH (0.5 mM) incubates in the absence of chelators with and without added CuZnSOD. Thus, other NO consumption pathways leading to products (e.g., $NO_2^-$, $NO_3^-$) must not be efficient compared to the RSNO producing pathways.

### 5.7.2 Mechanism of uncatalyzed NO transfer

Does uncatalyzed NO transfer involve formation of a nitroxyl disulfide intermediate (eq 1.15) or is NO released from the donor to give free NO which is then taken up by the acceptor? The reaction between SNAP and GSH in the presence of 1 mM DTPA does not go to completion since Figure 2.2 shows 0.87 mM SNAP and 1.07 mM GSNO at equilibrium. However, the NO-transfer efficiency between the thiols is close to 100% (Table 5.1). The NO-electrode measurements show the same level of free NO (~ 1 μM) in 0.5 mM SNAP/0.1 mM DTPA solutions with or without 0.5 mM GSH (Figure 2.13 curve c *vs* Figure 2.14 curve b). This indicates that GSH does not promote release of free NO from SNAP. When only SNAP is present the amount of free NO is determined by the equilibrium in reaction 5.19. Once GSH is added, it can react with $NAP^{\cdot}$ (eq 5.20) to yield NAP and $GS^{\cdot}$. The latter can react with $NO^{\cdot}$ to give GSNO and the equilibrium in eq 5.20 is moved to the right consuming SNAP and producing GSNO:

$$SNAP \rightleftharpoons NO^{\bullet} + NAP^{\bullet} \quad (5.19)$$

$$NAP^{\bullet} + GSH \rightleftharpoons NAP + GS^{\bullet} \quad (5.20)$$

$$NO^{\bullet} + GS^{\bullet} \rightleftharpoons GSNO \quad (5.21)$$

Once GSNO formed, will decompose releasing NO in a similar manner as SNAP and will push the reaction 5.19 to the SNAP formation:

$$GSNO \rightleftharpoons NO^{\bullet} + GS^{\bullet} \quad (5.22)$$

Thus, efficient NO transfer can involve concerted nucleophilic attack of $GS^-$ on SNAP (eq 1.15) and/or reactions 5.19-5.22. In the latter case the equilibrium constant of the trans-S-nitrosation reaction (eq. 5.1) is the sum of the equilibrium constants of reactions 5.19-5.22. The more stable RSNO in solution will be the main product. However, under the present conditions trapping of $NO^{\cdot}$ by $GS^{\cdot}$ has to be more efficient than $GS^{\cdot}$ dimerization to GSSG. The lack of GSSG ions in the mass spectrum in Figure 2.11 support this hypothesis.

Recently, NO transfer from RSNOs to N-methylaniline was examined (21). The authors used 10-100-fold excess RSNO over NO acceptor, and the presence of EDTA completely halted the reaction. When the reactants were present in an equimolar ratio, in the absence of chelators, the products were 50% of the N-nitrosated species and 50% nitrite. The authors suggest that copper-catalyzed decomposition of the RSNO and the free NO generated under aerobic condition formed $N_2O_3$ (21), a powerful nitrosating

agent that also undergoes hydrolysis to $NO_2^-$ (eq 1.3). Since the RSNO/N-methylaniline reactions were completely halted in the presence of a chelator, but not the RSNO/R'SH reactions studied here (e.g., Figure 2.2), the reaction of RS$^\cdot$ radicals with N-methylaniline (the equivalent of eq 5.20) may not be efficient, and/or concerted nucleophilic attack of the aniline on RSNO may not lead to NO transfer (eq. 1.15).

The difference in reactants/products ratio at equilibrium of catalyzed *vs.* uncatalysed processes (Figure 2.2 *vs.* 2.4) proves the presence of two different reactions. If the catalyzed mechanism can be completely halted by removing traces of cooper, the uncatalysed can not be stopped.

### 5.7.3 Suggestions for future studies

1. Because all reactions were carried out in air-saturated buffers, the effects of removing $O_2$ should be examined. The sensitivity to $O_2$ will depend on thiol concentration and should affect the NO transfer efficiency at lower concentrations.

2. The ESI-MS analysis of SNAP/GSH mixtures after 5 min incubation should be investigated to confirm the products formed.

3. Fluorescence changes *vs* time were monitored here only for GSNO/d-hCys. The changes in SNAP/d-hCys incubates should be probed by fluorescence to compare the results with the SNAP/GSH and GSNO/d-hCys data reported here.

4. The unexpected effects of neocuproine on the fluorescence of GSNO/d-hCys incubates should be elucidated.

## *Bibliography*


(1) Cullota, E.; Koshland, D. E.; (1992) *Science 258*, 1862

(2) Hou, Y-C.; Janczuk, A. and Wang P.G.; (1999) *Curr Pharma Design 5*, 417-441

(3) Williams, D.L.H.; (2003) *Org Biomol Chem 1*, 441-449

(4) Oae, S.; Shinhama, K.; (1983) *Org Prep Proc Int 15*, 165-198

(5) Lu, J.-M.; Wittbrodt, J. M.; Wang, K.; Wen, Z.; Schlegel, H.B.; Wang, P. G. and Cheng, J.-P.; (2001) *J Am Chem Soc 123*, 2903-2904

(6) Wang, P. G.; Xiang, M.; Tang, X.; Wu, X.; Wen, Z.; Cai, T. and Janczuk A.; (2002) *J Am. Chem Soc 102,* 1091-1134

(7) Lee, J.; Chen, L.; West, A. H. and Richter-Addo, G.B.; (2002) *Chem Rev 102*, 1019-1065

(8) Williams, D. L. H.; (1999) *Acc Chem Res 32*, 869-876

(9) Hogg, N.; (1999) *Anal Biochem 272*, 257-262

(10) Tao, L. and English, A. M.; (2004) *Biochemistry 43*, 4028-4038

(11) Dicks, A. P. and Williams, D. L. H.; (1996) *Chem Biol 3*, 655-659

(12) Bertini, I.; Gray, H. B.; Lippard, S. J. and Valentine, J. S.; (1994) *Bioinorg Chem,* 298-313

(13) Ramachandran, N.; Jacob, S.; Zielinski, B.; Curatola, G.; Mazzanti, L. and Mutus, B.; (1999) *Biochim Biophys Acta 1430*, 149-154

(14) Gros, C. and Labouesse B.; (1968) *Euro J Biochem 7*, 463-470

(15) Barnett, D.J.; McAninly, J. and Williams, D. L. H.; (1994) *J Chem Soc Perkin Trans 2*, 1131-1133

(16) Dicks, A.P.; Li, E.; Munro, A.P.; Swift, H. R. and Williams, D. L. H.; (1998) *Can J Chem 76*, 786-794

(17) Romeo, A. A.; Capobianco, J. A. and English, A.; (2001) *J Biol Chem 27*, 24135-24141

(18) Tao, L. and English, A. M.; (2003) *Biochem 42*, 3326-3334

(19) Arnelle, D. R. and Stamler, J.; (1995) Arch Biochem *Biophys 318*, 279-285

(20) Wang, K.; Wen, Z.; Zhang, W.; Xian, M.; Cheng, J. and Wang, G.; (2000) *Bio Med Chem Lett 11*, 433-436

(21) Noble, R. D. and Williams, H. L. D.; (2002) *J Chem Soc Perkin Trans 2*, 1834-1838

(22) Noble, R. D.; Swift, R. H. and Williams, D. H. L.; (1999*) Chem Commun,* 2317-2318

(23) Bartberger, M. D.; Houk, K. N.; Powell, S. C.; Mannion, J. D.; Lo, K. Y.; Stamler, J. S. and Toone, E. J.; (2000) *J Am Chem Soc 122*, 5889-5890

(24) Ramachandran, N.; Root, P.; Jiang, X. M.; Hogg, P. J. and Mutus, B.; (2001) *Proc Natl Acad Sci U S A 98*, 9539-9544

(25) Chen, X.; Wen, Z.; Xian, M.; Wang, K.; Ramachandran, N.; Tang, X.; Schlegel, H. B.; Mutus, B. and Wang, P. G.; (2001) *J Org Chem 66*, 6064-73

(26) Rossi, R.; Lusini, L.; Giannerini, F.; Giustarini, D.; Lungarella, G. and Di Simplicio, P.; (1997) *Anal Biochem 254*, 215-220

(27) Stubauer, G.; Giuffre, A. and Sarti, P.; (1999) *J Biol Chem 40*, 28128-28133

(28) Williams, D. L. H.; (1996) *Chem Soc Chem Commun*, 1085-1091

(29) Gorren, A.C.F.; Schrammel, A.; Schmidt, K. and Mayer, B.; (1996) *Arch. Biochem Biophys 330*, 219-228

(30) Hardvey, D.; Smith, G. F.; (1966) *The copper reagents: cuproine, neocuproine, bathocuproine,* 16-25

(31) Noble, D.R. and Williams, H. L. D.; (2000) *Nitric Oxide 4*, 392-398

(32) Jourd'heuil, D.; Laroux, F. S.; Miles, A. M.; Wink, D. A. and Grisham, B. M.; (1999) *Arcae Biochem Bioph 361*, 323-330

(33) Lagunoff, D. and Ottolenghi, P.; (1966) *Compt Rend Trav Lab Carlsberg 4*, 63-83

(34) Xiang, M.; Chen, X.; Liu, Z.; Wang, K. and Wang, G. P.; (2000) *J Biol Chem 275*, 20467-20473

(35) Chang, R.; (1986) *General Chemistry,* 720-721

(36) James, B. R. and Williams, R. J. P.; (1961) *J. Chem. Soc. II*, 2007-2019

(37) Houk, K. N.; Hietbrink, N. B.; Bartberger. D. M.; McCarren, P. R.; Choi, B. Y.; Voyksner, R. D.; Stamler, J. S. and Toone, J. E.; (2003) *J Am Chem Soc 125*, 6972-6976

(38) Zhang, X. and Broderick, M.; (2000) *Mod Asp Immunobiol* 4, 160-165

(39) Barnett, J. D.; Rios, A. and Williams, H. D. L.; (1995) *Chem Soc Perkin Trans 2*, 1279-1282